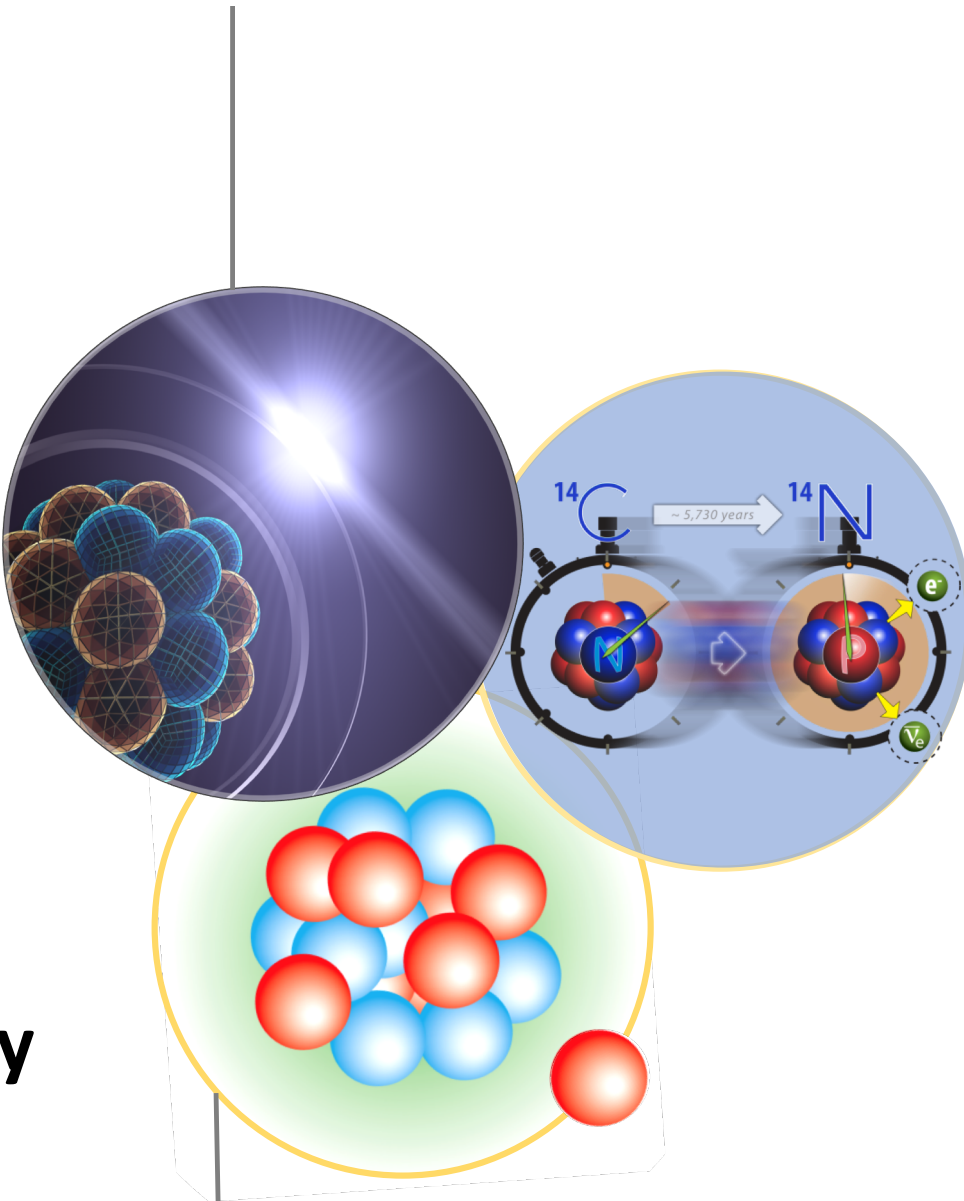


Recent advances in coupled-cluster computations of nuclei

Gaute Hagen
Oak Ridge National Laboratory

Progress in Ab Initio Nuclear Theory

TRIUMF, Vancouver March 2nd, 2023



Collaborators

@ ORNL / UTK: **B. Acharya, T. Djärv, B. Hu, G. R. Jansen, Z. H. Sun, T. Papenbrock**

@ CEA/Saclay: T. Duguet

@ Chalmers: A. Ekström, C. Forssén

@ Mainz: **F. Bonaiti, S. Bacca, W. G. Jiang, J. E. Sobczyk**

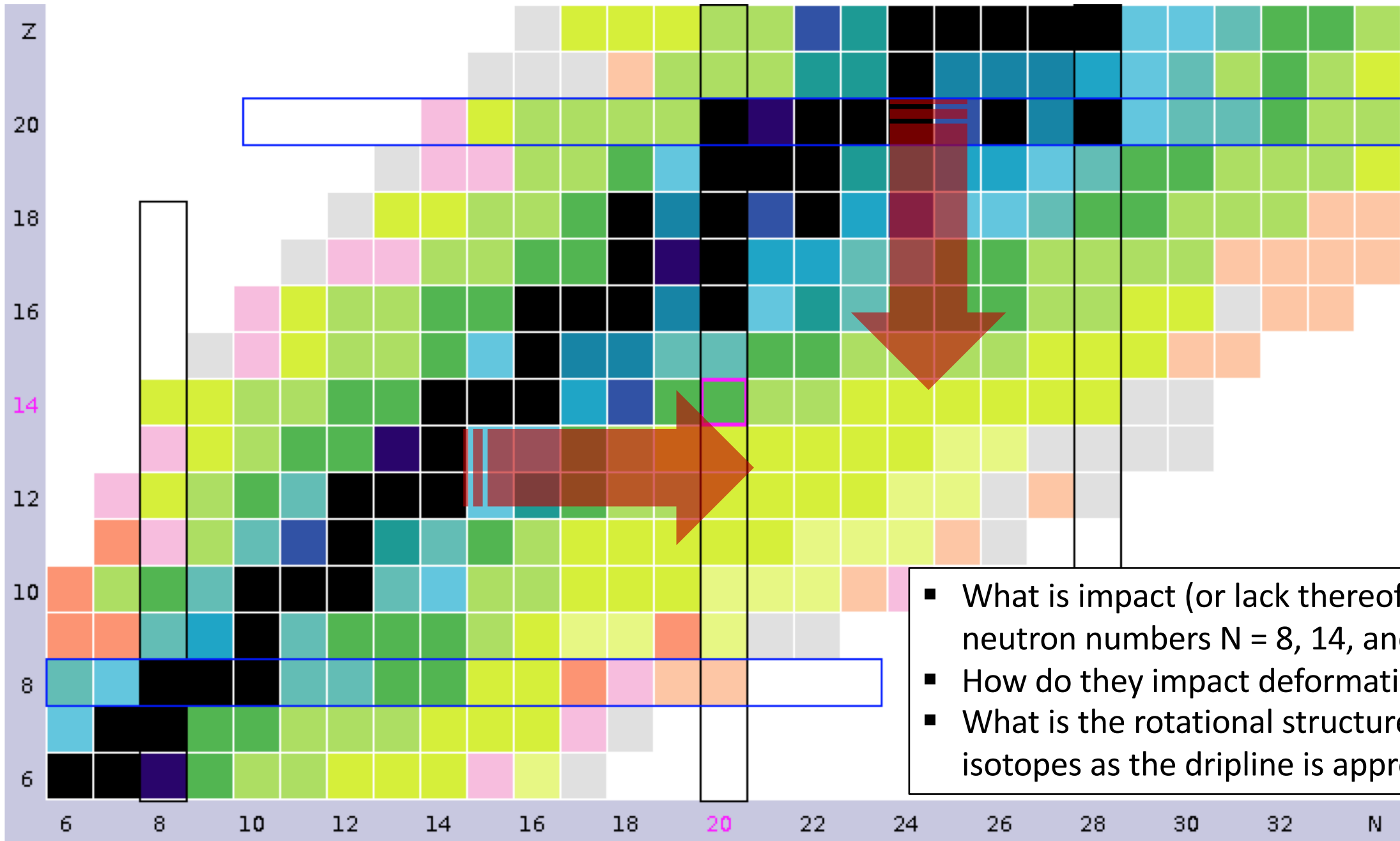
@ ND: S. R. Stroberg

@ LANL: S. Gandolfi, D. Lonardoni, **S. Novario**

@ TRIUMF: **P. Gysbers, J. Holt, P. Navratil**

@ TU Darmstadt: **T. Miyagi, A. Tichai**

Coupled-cluster computations of deformed nuclei

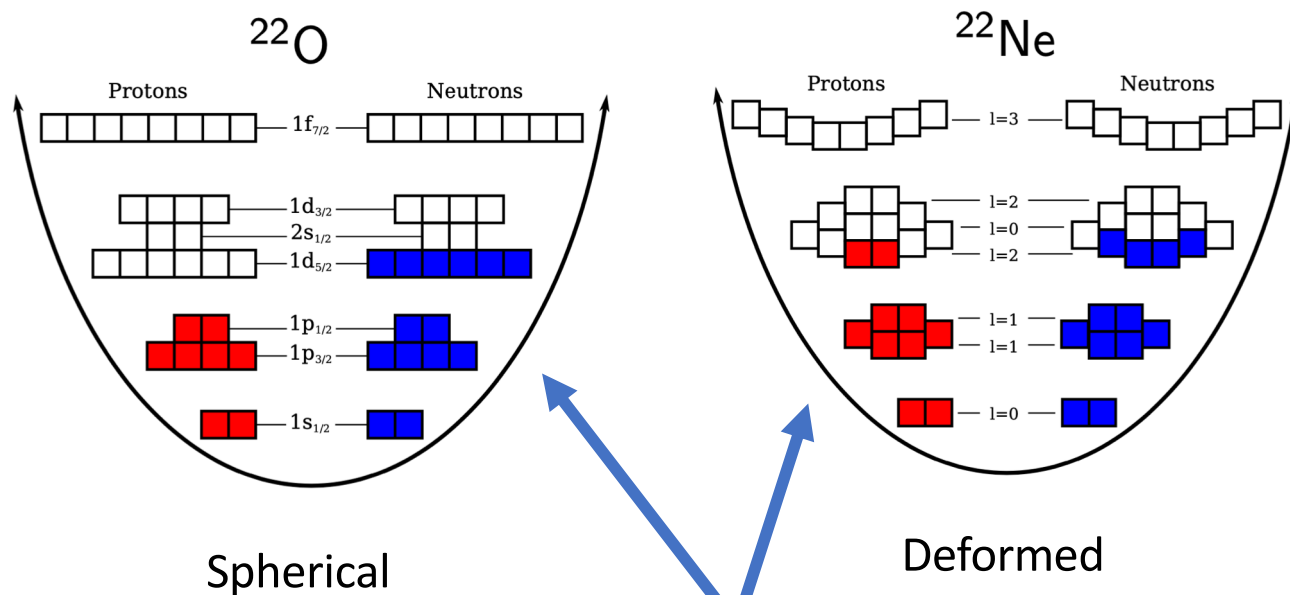


- What is impact (or lack thereof) of the “magic” neutron numbers $N = 8, 14,$ and 20 on structure?
- How do they impact deformation past $N = 20$?
- What is the rotational structure of neutron-rich isotopes as the dripline is approached?

Coupled-cluster computations of deformed nuclei

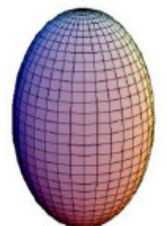
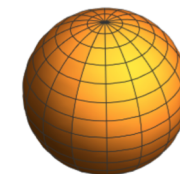
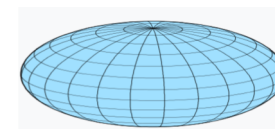
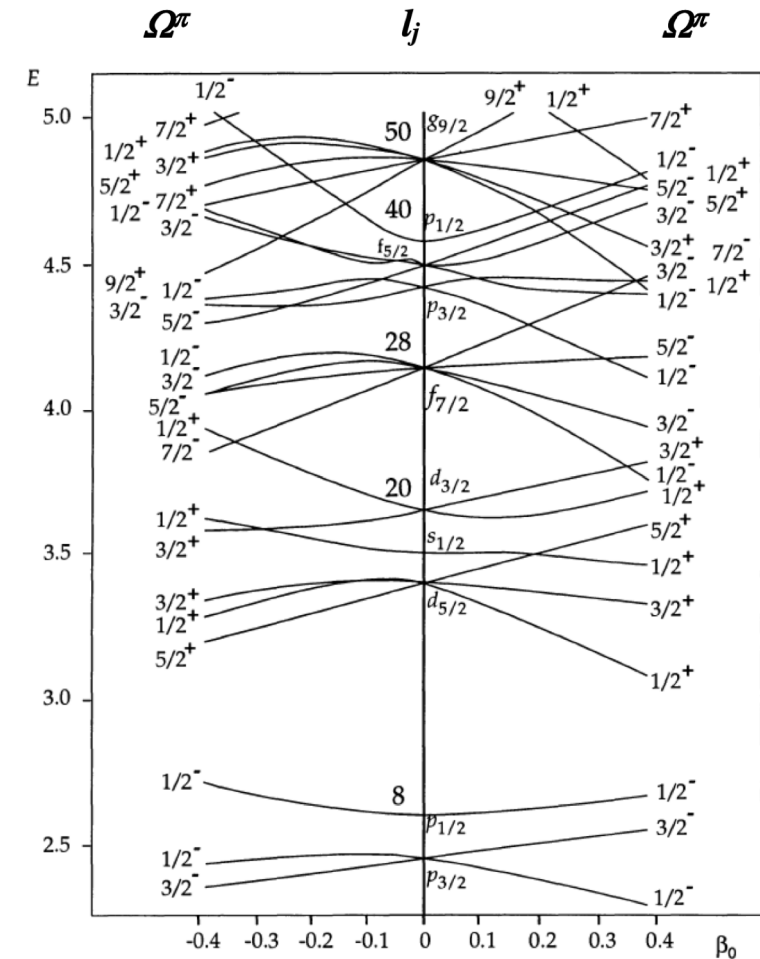
The key lies in choosing the correct starting point

Wave-function based methods starts from a mean-field reference state



$$|\Psi\rangle = \Omega |\Phi\rangle$$

Wave-operator (includes many-body correlations)



Coupled-cluster method

$$\Psi = e^T |\Phi\rangle$$

$$T = T_1 + T_2 + \dots$$

$$T_1 = \sum_{ia} t_i^a a_a^\dagger a_i \quad T_2 = \frac{1}{4} \sum_{ijab} t_{ij}^{ab} a_a^\dagger a_b^\dagger a_j a_i$$

$$\bar{H}_{\text{CCSD}} = \begin{pmatrix} \text{0p0h} & \text{1p1h} & \text{2p2h} \\ E_{\text{CCSD}} & \bar{H}_{0S} & \bar{H}_{0D} \\ 0 & \bar{H}_{SS} & \bar{H}_{SD} \\ 0 & \bar{H}_{DS} & \bar{H}_{DD} \end{pmatrix} \begin{matrix} \text{0p0h} \\ \text{1p1h} \\ \text{2p2h} \end{matrix}$$

$$E = \langle \Phi | \bar{H} | \Phi \rangle$$

$$0 = \langle \Phi_i^a | \bar{H} | \Phi \rangle$$

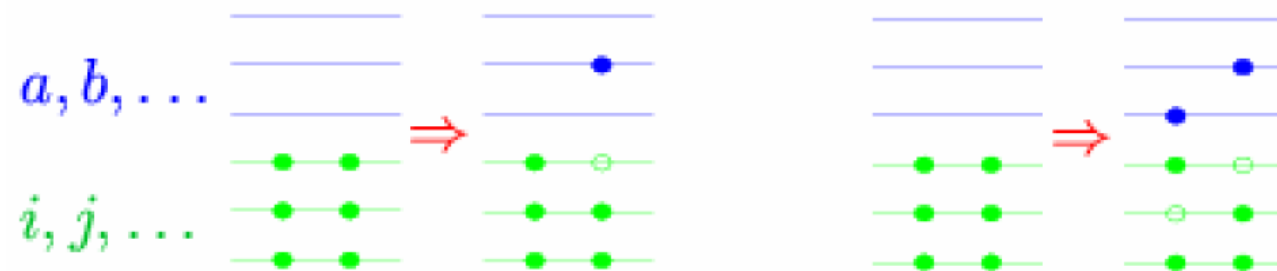
$$0 = \langle \Phi_{ij}^{ab} | \bar{H} | \Phi \rangle$$

$$\bar{H} \equiv e^{-T} H e^T = (H e^T)_c = \left(H + H T_1 + H T_2 + \frac{1}{2} H T_1^2 + \dots \right)_c$$

- ☺ Scales gently (polynomial) with increasing system size
- ☺ Truncation is only approximation
- ☺ Fulfills a bi-variational principle
- ☺ A lot of freedom in the choice of reference state (spherical, deformed, pairing,...)

CCSD generates similarity transformed Hamiltonian with no 1p-1h and no 2p-2h excitations

Correlations are *exponentiated* 1p-1h and 2p-2h excitations. Part of Ap-Ah excitations included!



Coupled-cluster computations of deformed nuclei

1. Compute Hartree-Fock reference state
 - Nontrivial vacuum state informs us about emergent breaking of symmetries
 - Yields normal-ordered two-body Hamiltonian
2. Include dynamical (extensive) correlations via coupled-cluster theory
 - (or via IMSRG, or Gorkov methods, or Green's functions)
 - Cost increases polynomial with mass number
3. Perform symmetry projections
 - Non-extensive contributions to the energy
 - Often relevant for transition matrix elements

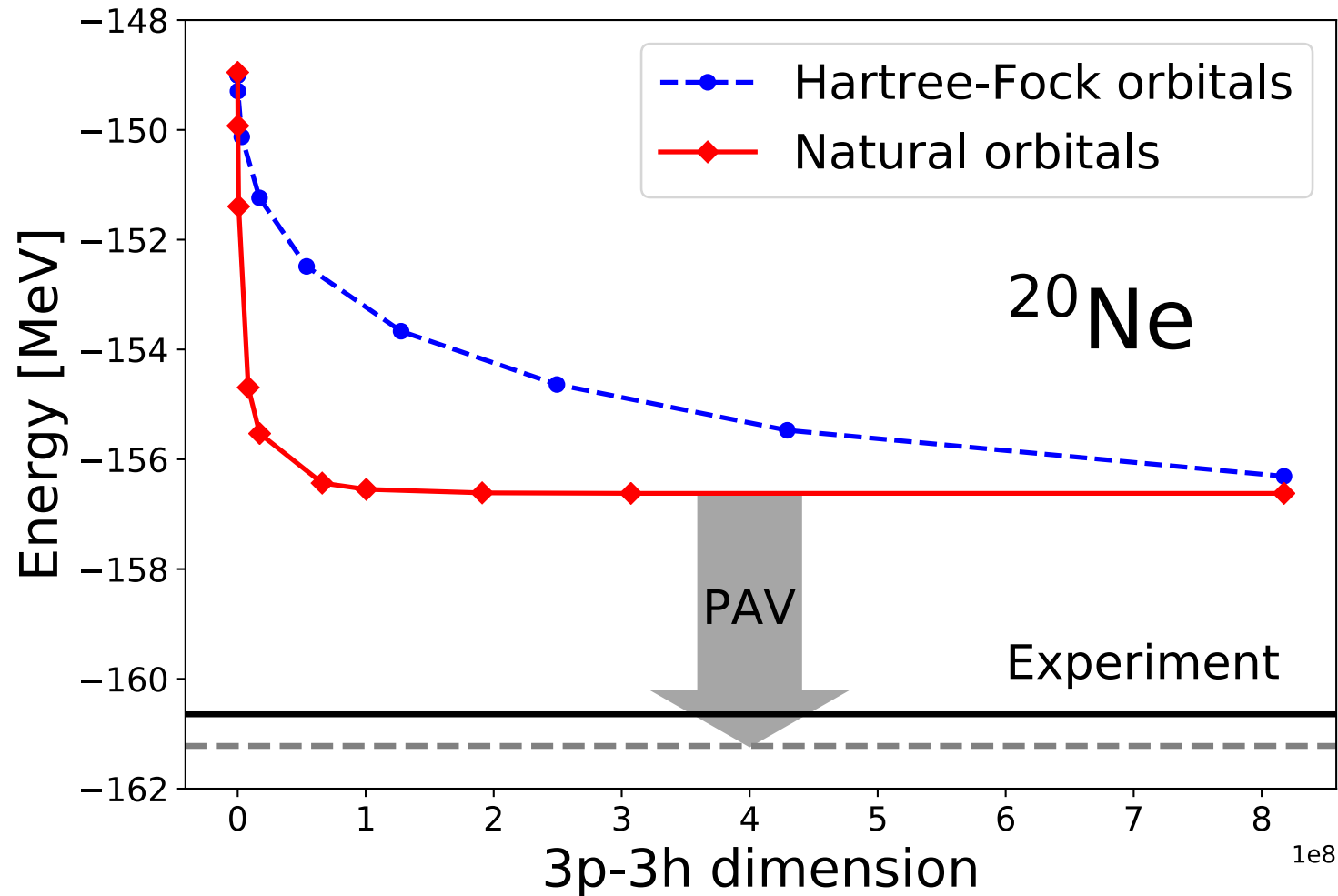
The total energy of
a nucleus

Dynamic correlation (large contribution
and requires size-extensive methods)

Static correlation (can use
non size-extensive methods)

$$E = E_{\text{ref}} + \Delta E_{\text{CC}} + \delta E$$

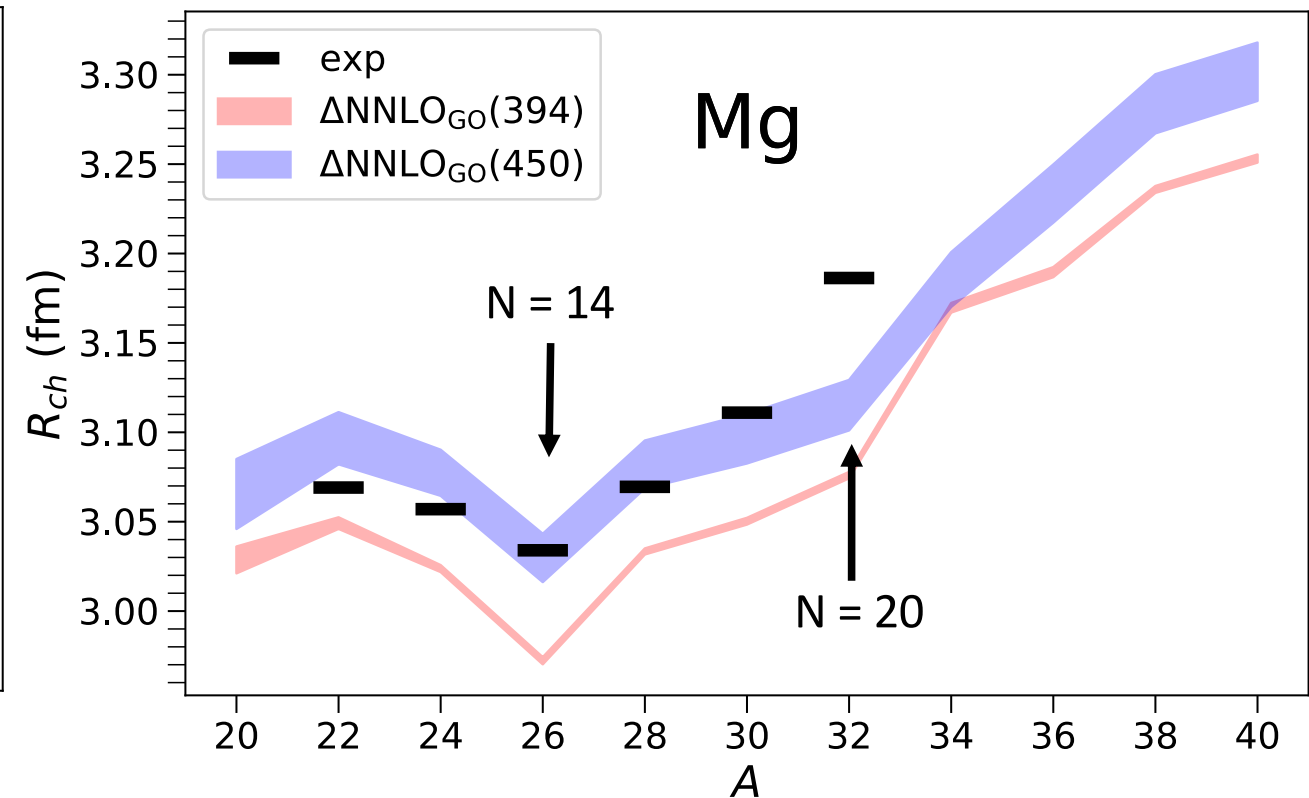
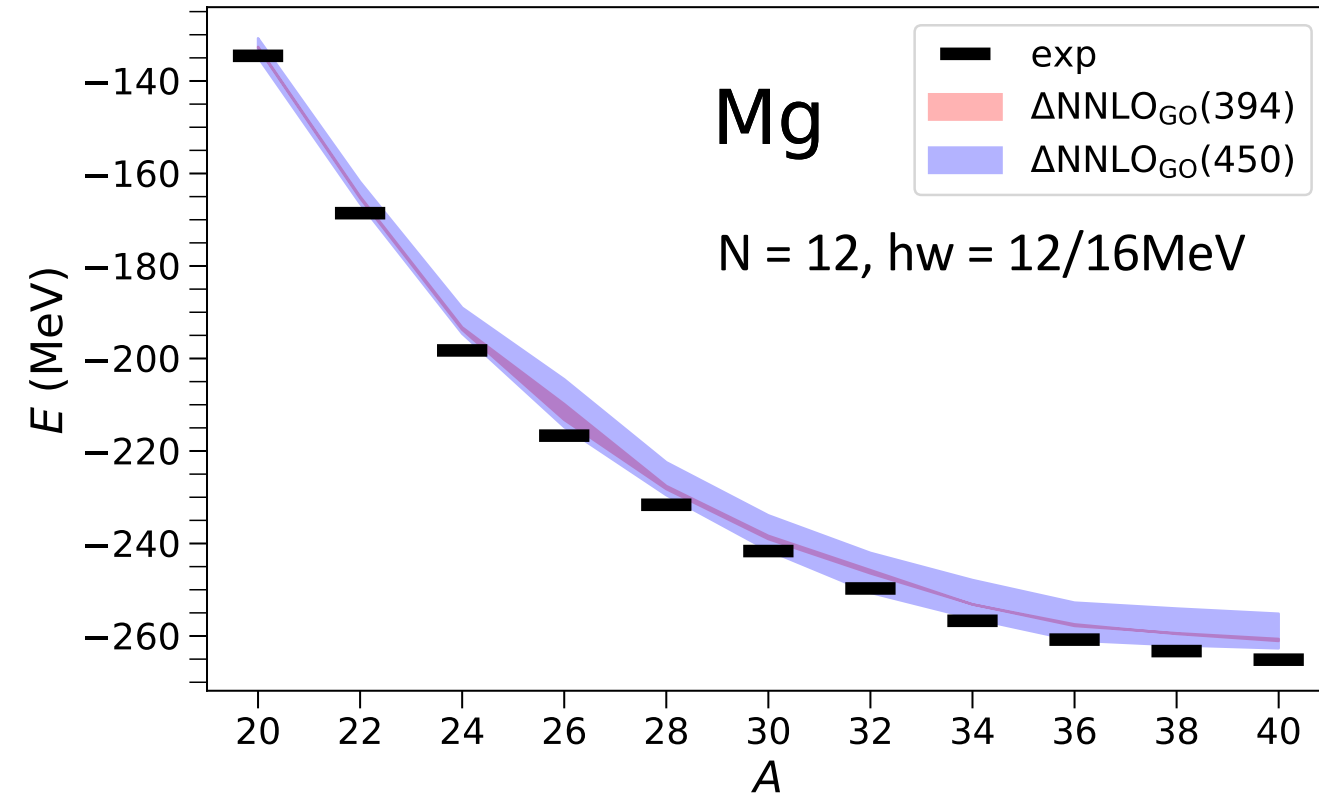
Coupled-cluster computations of deformed nuclei – natural orbitals



- Coupled-cluster calculations from axially symmetric reference states
- Natural orbitals from many-body perturbation theory [A. Tichai, et al PRC (2019)] yields rapid convergence with respect 3p3h excitations in CCSDT-1
- Hartree-Fock with projection after variation (PAV) gives upper bound on the energy gain from symmetry restoration

Computations of magnesium isotopes

- Symmetry broken reference states allow us to address open-shell/deformed nuclei
- Dripline predicted at ^{40}Mg – continuum may impact the location of the dripline
- Charge radii predicts shell closures at $N = 8$, $N = 14$, and at $N = 20$
- The bands indicate uncertainties from model-space truncations



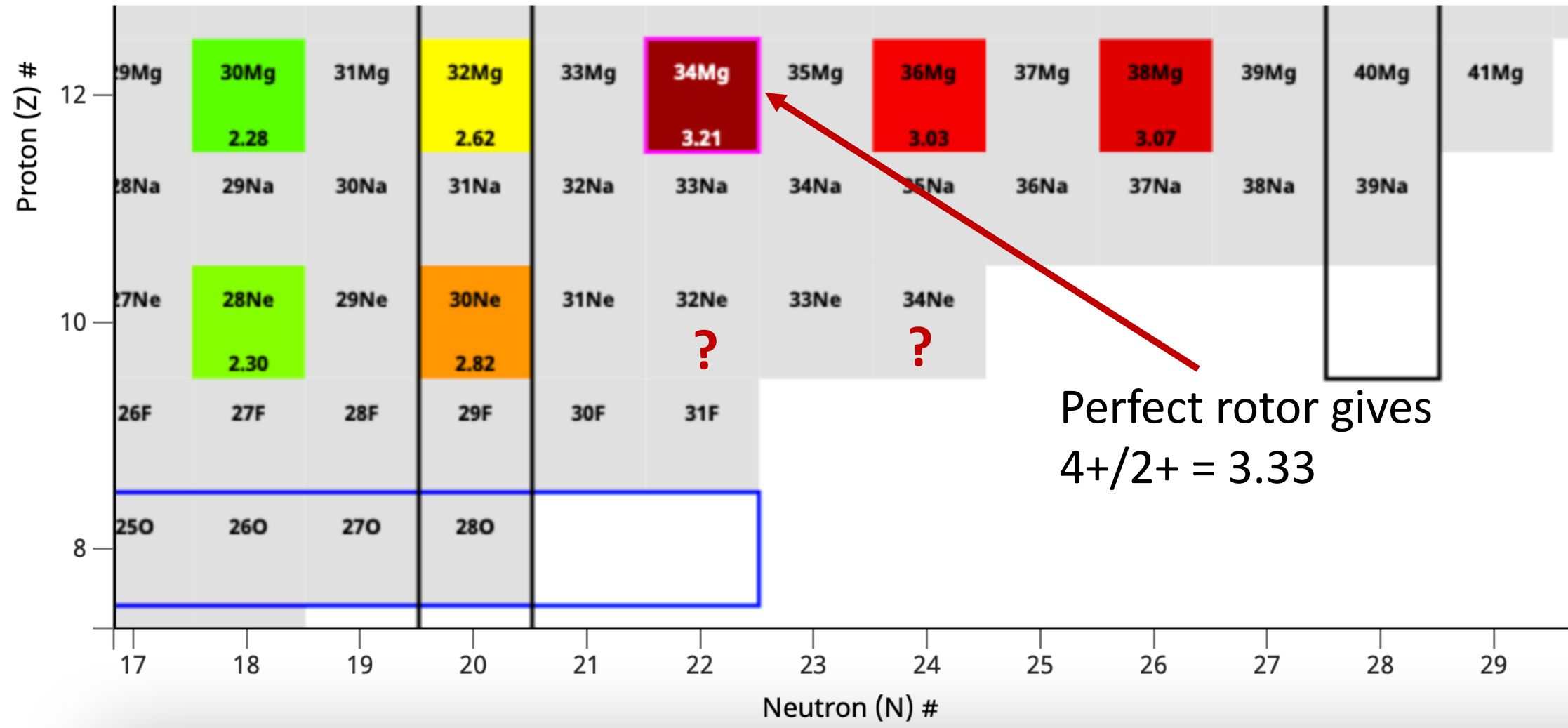
Impact of symmetry projection on radii

G. Hagen, S. J. Novario, Z. H. Sun, T. Papenbrock, G. R. Jansen, J. G. Lietz, T. Duguet, A. Tichai Phys. Rev. C 105, 064311 (2022)

	Unprojected			Projected				
	E	$\langle J^2 \rangle$	R_{ch} (fm)	δE	$E^{(0)} = E + \delta E$	R_{ch} (fm)	$E^{(2)} - E^{(0)}$	$E^{(4)} - E^{(0)}$
^{20}Ne								
HF	-59.442	22.778	2.623	-5.760	-65.202	2.619	1.26	4.34
SLD	-122.467	19.059	2.601	-4.332	-126.799	2.598	1.13	3.90
CCD	-142.666	16.128	2.621	-3.627	-146.293	2.620	1.19	3.68

	Unprojected			Projected				
	E	$\langle J^2 \rangle$	R_{ch} (fm)	δE	$E^{(0)} = E + \delta E$	R_{ch} (fm)	$E^{(2)} - E^{(0)}$	$E^{(4)} - E^{(0)}$
^{34}Mg								
HF	-85.687	24.740	2.727	-3.184	-88.87	2.724	0.67	2.29
SLD	-177.938	22.790	2.707	-2.479	-180.42	2.704	0.60	2.05
CCD	-221.315	20.213	2.725	-1.893	-223.21	2.722	0.53	1.69

Rotational structure of nuclei from ab-initio methods



Symmetry restored coupled-cluster theory

Projection after variation (PAV): $E^{(J)} = \frac{\langle \tilde{\Psi} | P_J H | \Psi \rangle}{\langle \tilde{\Psi} | P_J | \Psi \rangle}$

Right state is parametrized: $|\Psi\rangle = e^T |\Phi_0\rangle$

Left state is parametrized differently:

$\langle \tilde{\Psi} | = \langle \Phi_0 | (1 + \Lambda) e^{-T}$ or $\langle \tilde{\Psi} | = \langle \Phi_0 |$ or $\langle \tilde{\Psi} | = \langle \Psi |$

Bi-variational

Naïve

Hermitian

This talk

See Thomas Papenbrock's talk

$$P_J = \frac{1}{2} \int_0^\pi d\beta \sin(\beta) d_{00}^J(\beta) R(\beta)$$

$$R(\beta) \equiv e^{i\beta J_y}$$



Image credit: Wikimedia Commons

For axial symmetry around the z-axis the rotation operator is:

Symmetry restored coupled-cluster theory

The kernels can be evaluated by using Thouless theorem:

$$\langle \Phi_0 | R(\beta) = \langle \Phi_0 | R(\beta) | \Phi_0 \rangle \langle \Phi_0 | e^{V_1(\beta)}$$


$$\mathcal{H}(\beta) = \langle \Phi | \bar{R}(\beta) | \Phi \rangle \langle \Phi | Z(\beta) \tilde{H}(\beta) e^{V(\beta)} e^{T_2} | \Phi \rangle$$

$$\mathcal{N}(\beta) = \langle \Phi | \bar{R}(\beta) | \Phi \rangle \langle \Phi | Z(\beta) e^{V(\beta)} e^{T_2} | \Phi \rangle$$

Similarity transformed rotation operator and Hamiltonian:

$$\bar{R}(\beta) = e^{-T_1} R(\beta) e^{T_1}$$

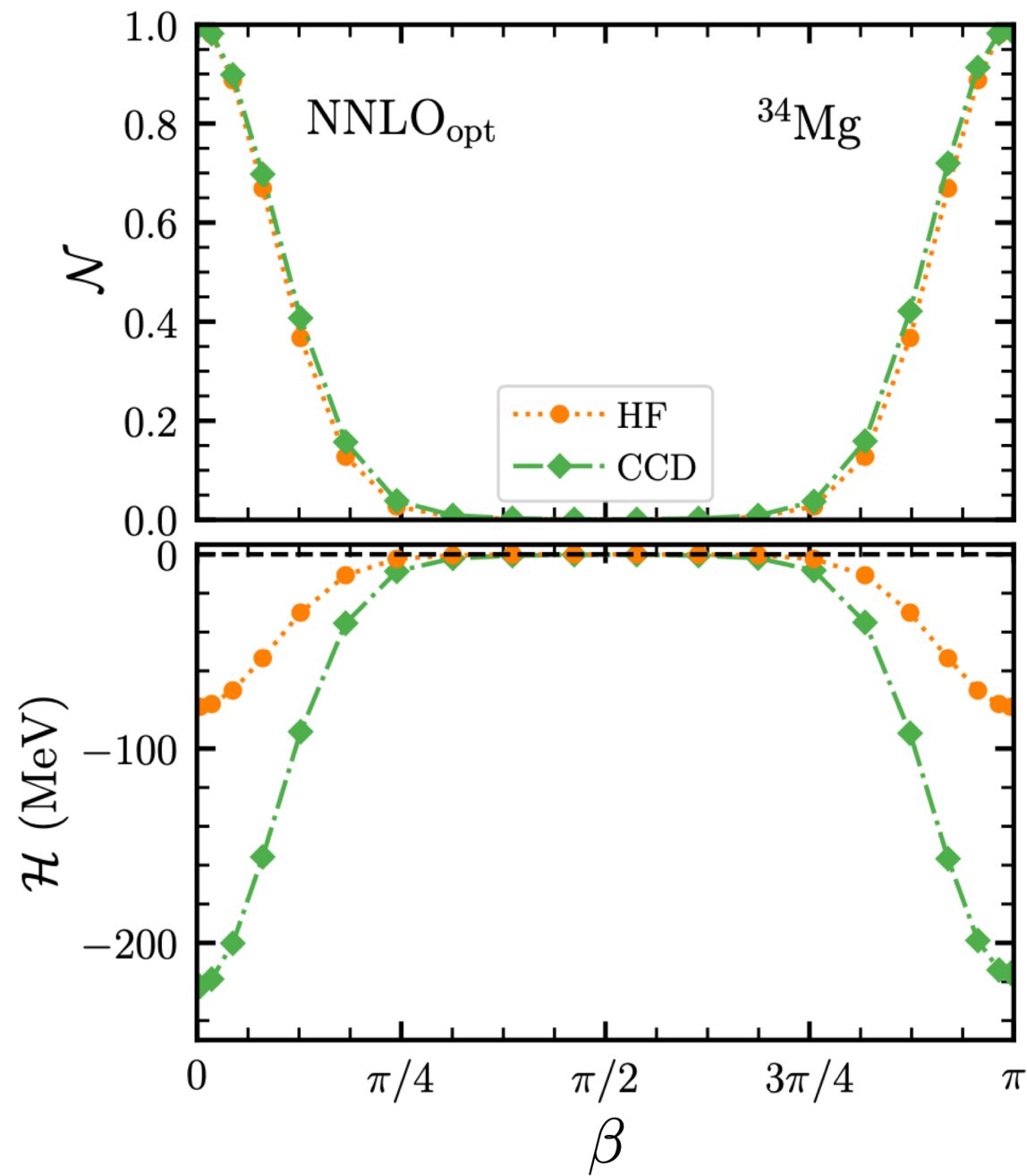
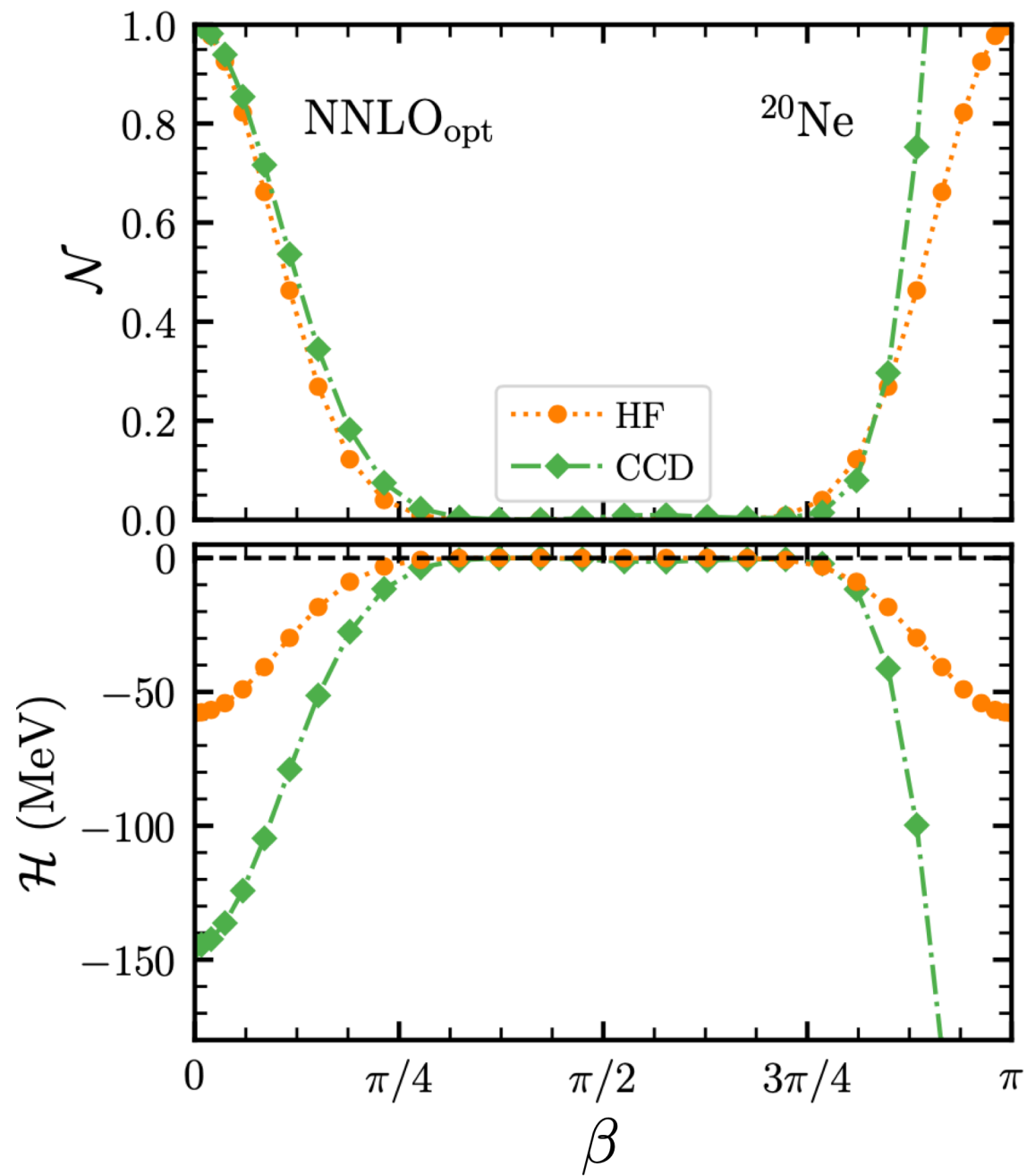
$$\tilde{H}(\beta) = e^{V_1(\beta)} \bar{H} e^{-V_1(\beta)}$$


$$e^{V(\beta)} e^{T_2} | \Phi \rangle = e^{W_0(\beta) + W_1(\beta) + W_2(\beta) + \dots} | \Phi \rangle$$

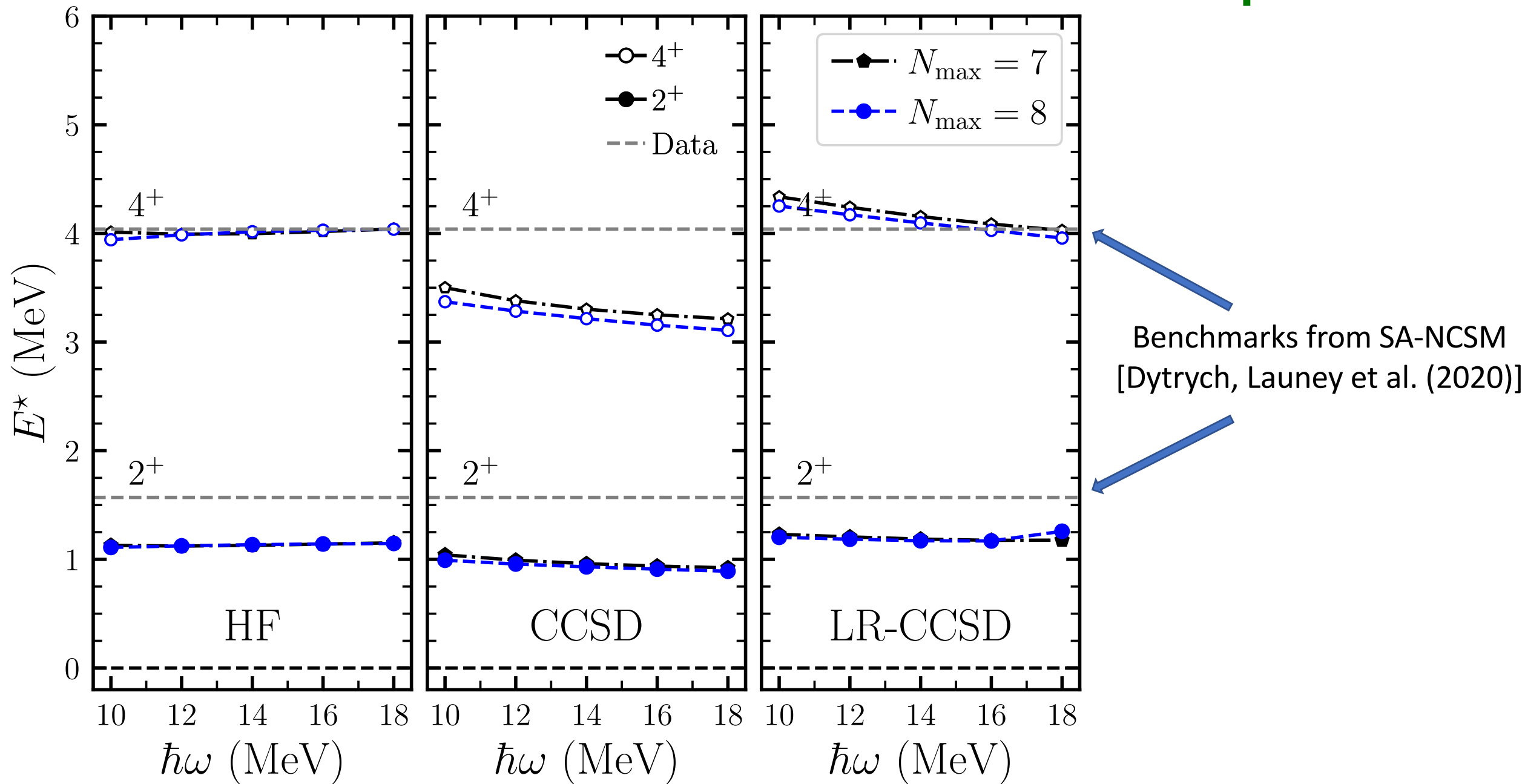
- Does not truncate
- Approximate restoration of symmetries
- Solve for disentangled amplitudes via ODEs

[see Qiu et al, J. Chem. Phys. 147, 064111 (2017)]

Disentangled versus HF energy and norm kernels

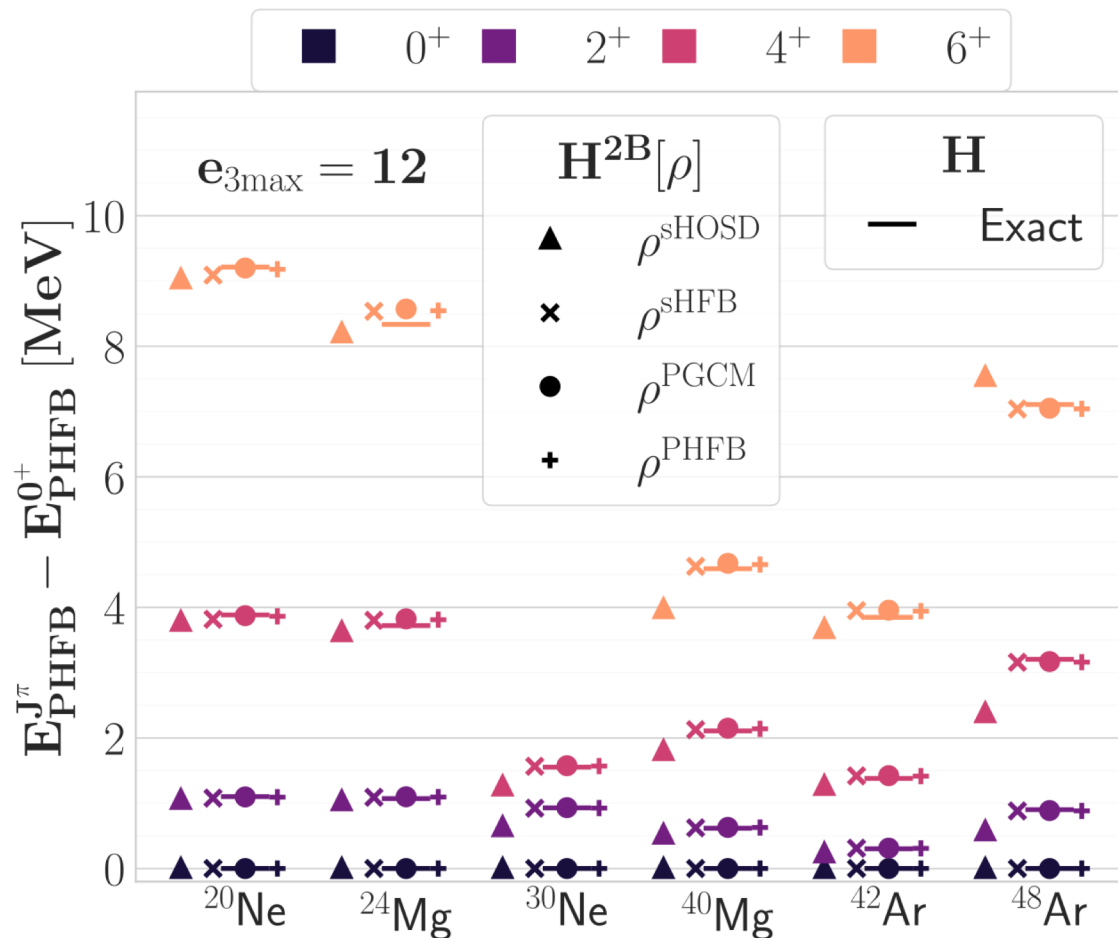


Projected bi-variational CCSD with NNLO_{opt} in ^{20}Ne



Inclusion of three-body forces

- The normal ordered 2-body approximation breaks rotational symmetry when normal-ordered with respect to a broken symmetry reference state
- Perform spherical Hartree-Fock with fractional filling to normal-order three-nucleon force
- Use normal-ordered Hamiltonian in the 2-body approximation in a second Hartree-Fock calculation of deformed nuclei



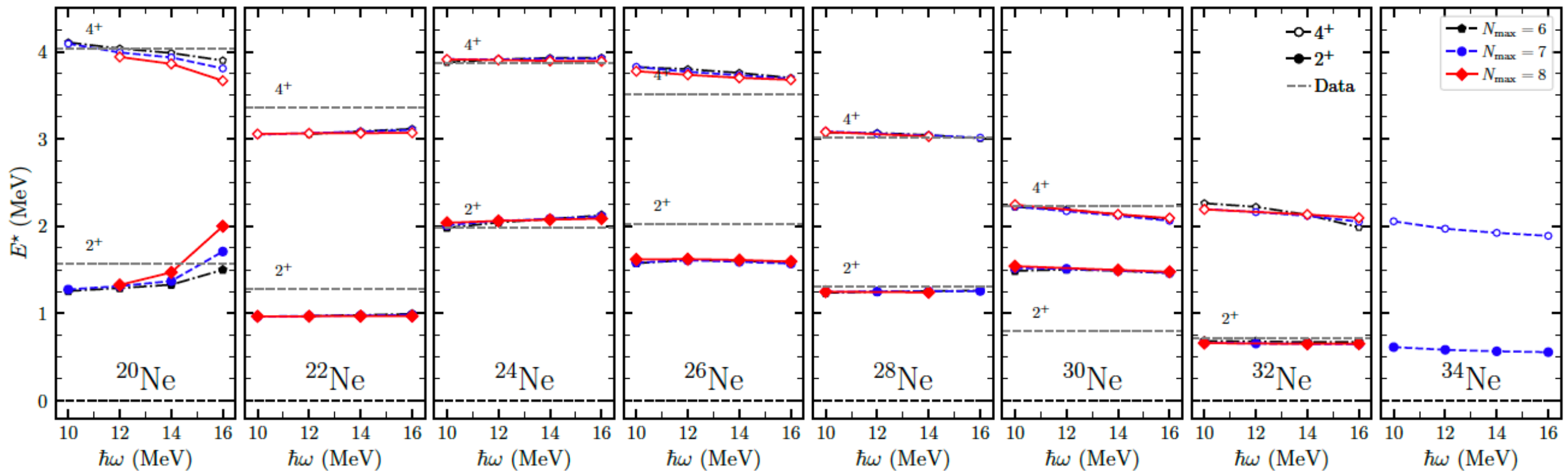
$$\bar{h}^{(0)}[\rho] \equiv \frac{1}{3!} w^{(3)} \cdot \rho^{\otimes(3)},$$

$$\bar{h}^{(1)}[\rho] \equiv t^{(1)} - \frac{1}{2!} w^{(3)} \cdot \rho^{\otimes(2)},$$

$$\bar{h}^{(2)}[\rho] \equiv v^{(2)} + w^{(3)} \cdot \rho,$$

Neon isotopes: Inclusion of three-body forces and more accurate left state

Rotational structure of neutron-rich neon isotopes in good agreement with data

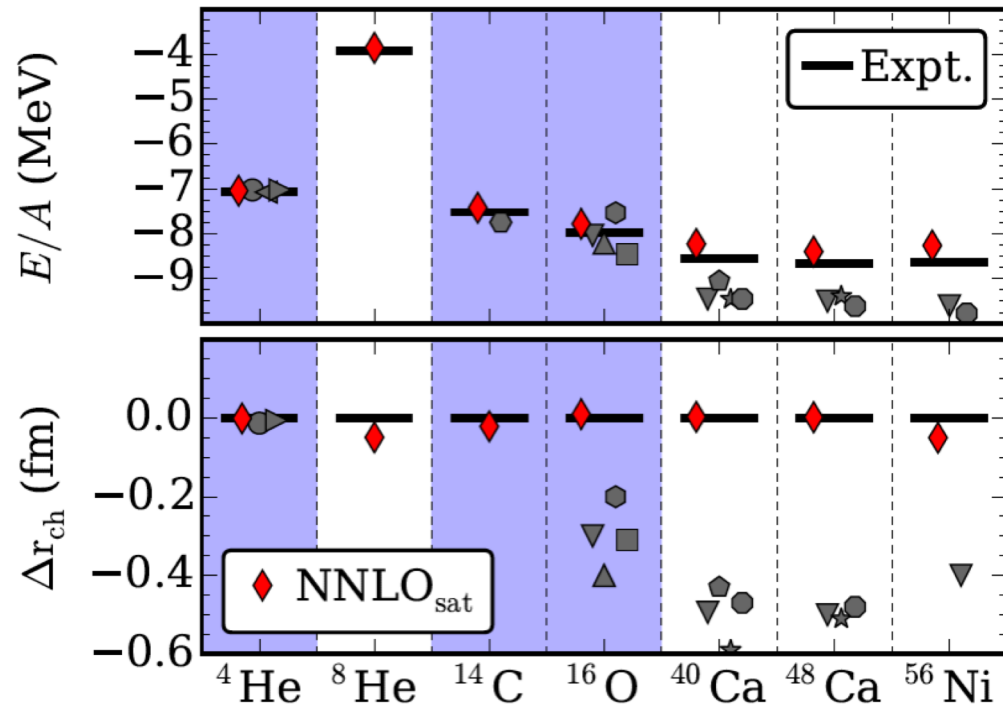


Interaction 1.8/2.0(EM) from Hebeler et al (2012) over-emphasizes $N=20$ shell closure

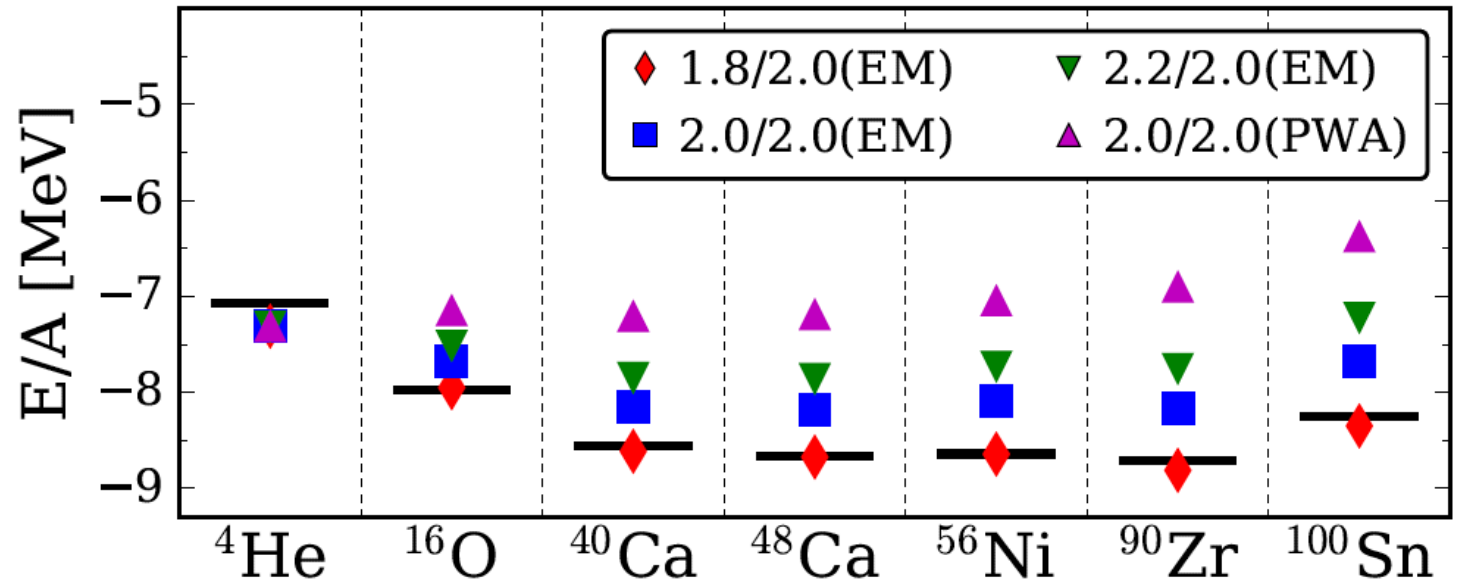
$^{32,34}\text{Ne}$ are as rotational as ^{34}Mg

PRELIMINARY

Why do some interaction models “work” better than others?



A. Ekström *et al*, Phys. Rev. C **91**, 051301(R) (2015).



K. Hebeler *et al* PRC (2011).

T. Morris *et al*, PRL (2018).

To answer this we need predictions with rigorous **uncertainty quantification** and **sensitivity analyses** that are grounded in the description of the underlying nuclear Hamiltonian

Global sensitivity analysis

Sensitivity analysis addresses the question ‘How much does each model parameter contribute to the uncertainty in the prediction?’

Global methods deal with the uncertainties of the outputs due to input variations over the whole domain.

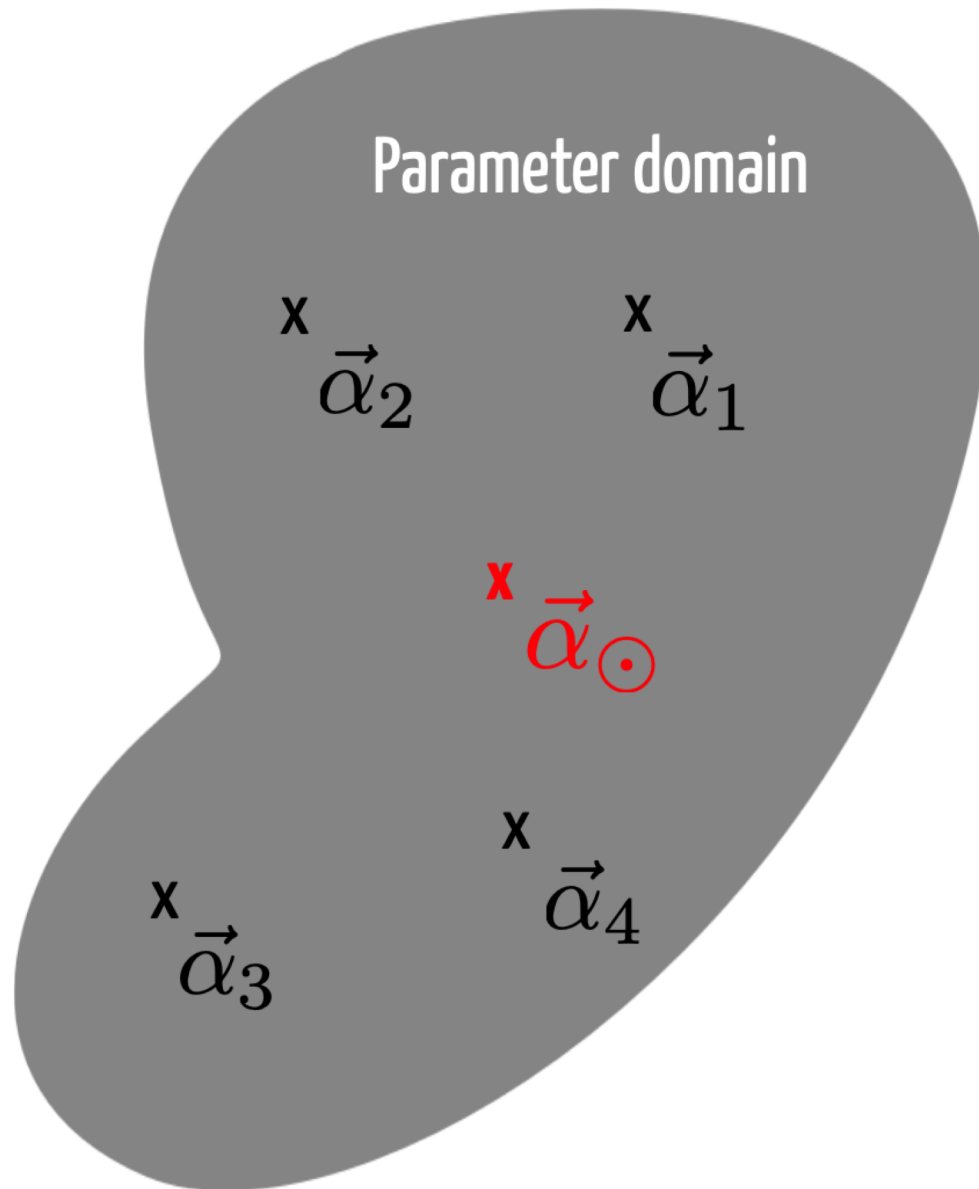
Computational bottleneck

A global sensitivity analysis of properties of atomic nuclei typically would require more than one million model evaluations



Emulating ab-initio coupled-cluster calculations

Andreas Ekström, Gaute Hagen PRL **123**, 252501 (2019)



- Eigenvector continuation method [Frame D. et al., Phys. Rev. Lett. 121, 032501 (2018), S. König et al Phys. Lett. B 810 (2020) 135814]
- Write the Hamiltonian in a linearized form

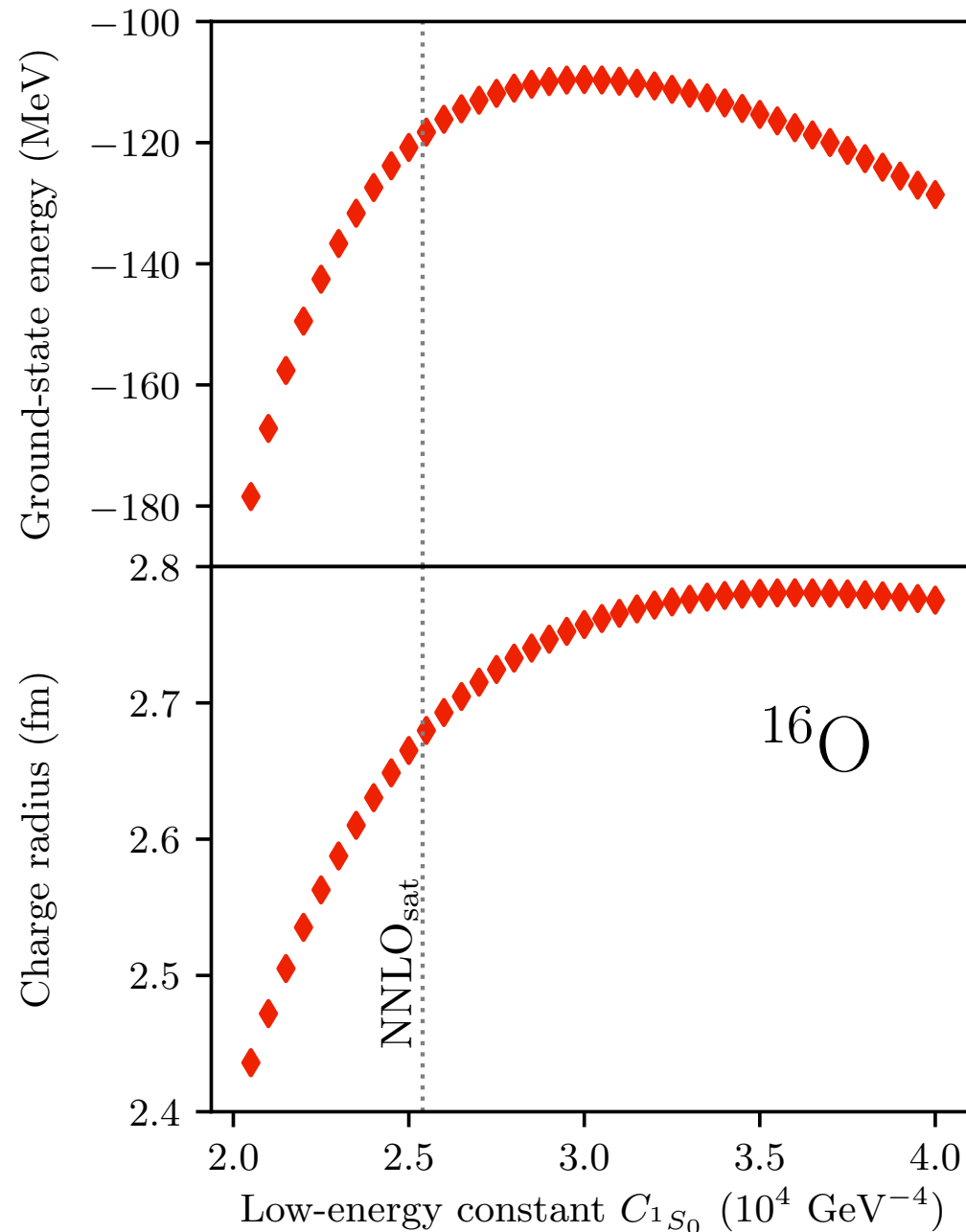
$$H(\vec{\alpha}) = \sum_{i=0}^{N_{\text{LECS}}=16} \alpha_i h_i$$

- Select “training points” where we solve the exact problem
- Project a target Hamiltonian onto subspace of training vectors and diagonalize the generalized eigenvalue problem

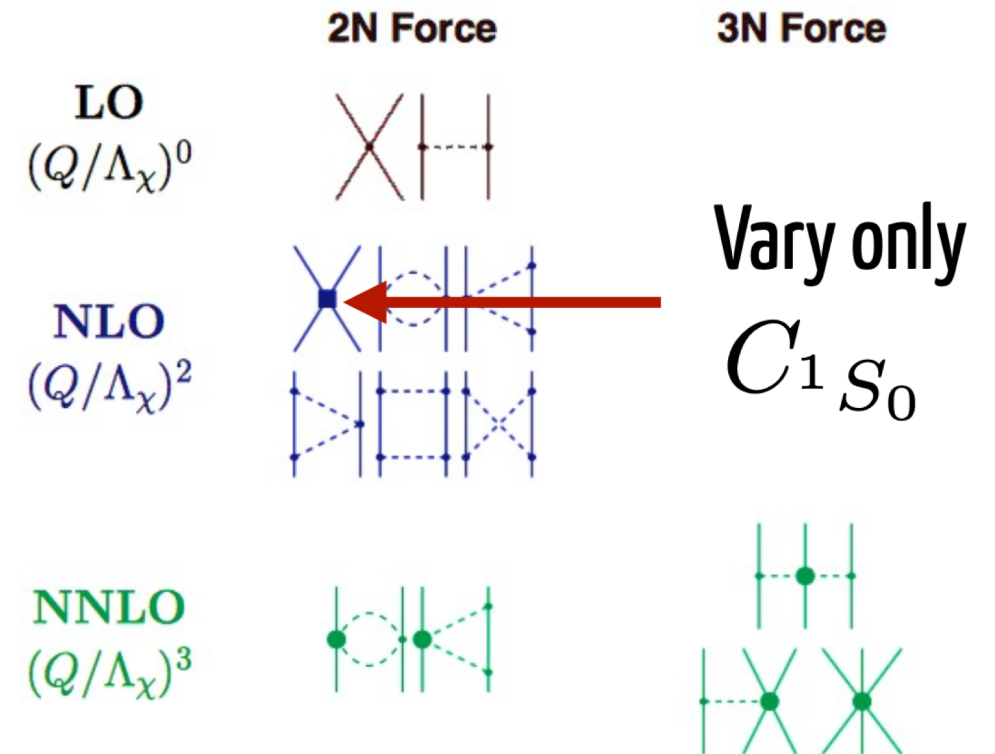
$$\mathbf{H}(\vec{\alpha}_{\odot}) \vec{c} = E(\vec{\alpha}_{\odot}) \mathbf{N} \vec{c},$$

Emulating ab-initio coupled-cluster calculations

Andreas Ekström, Gaute Hagen PRL **123**, 252501 (2019)

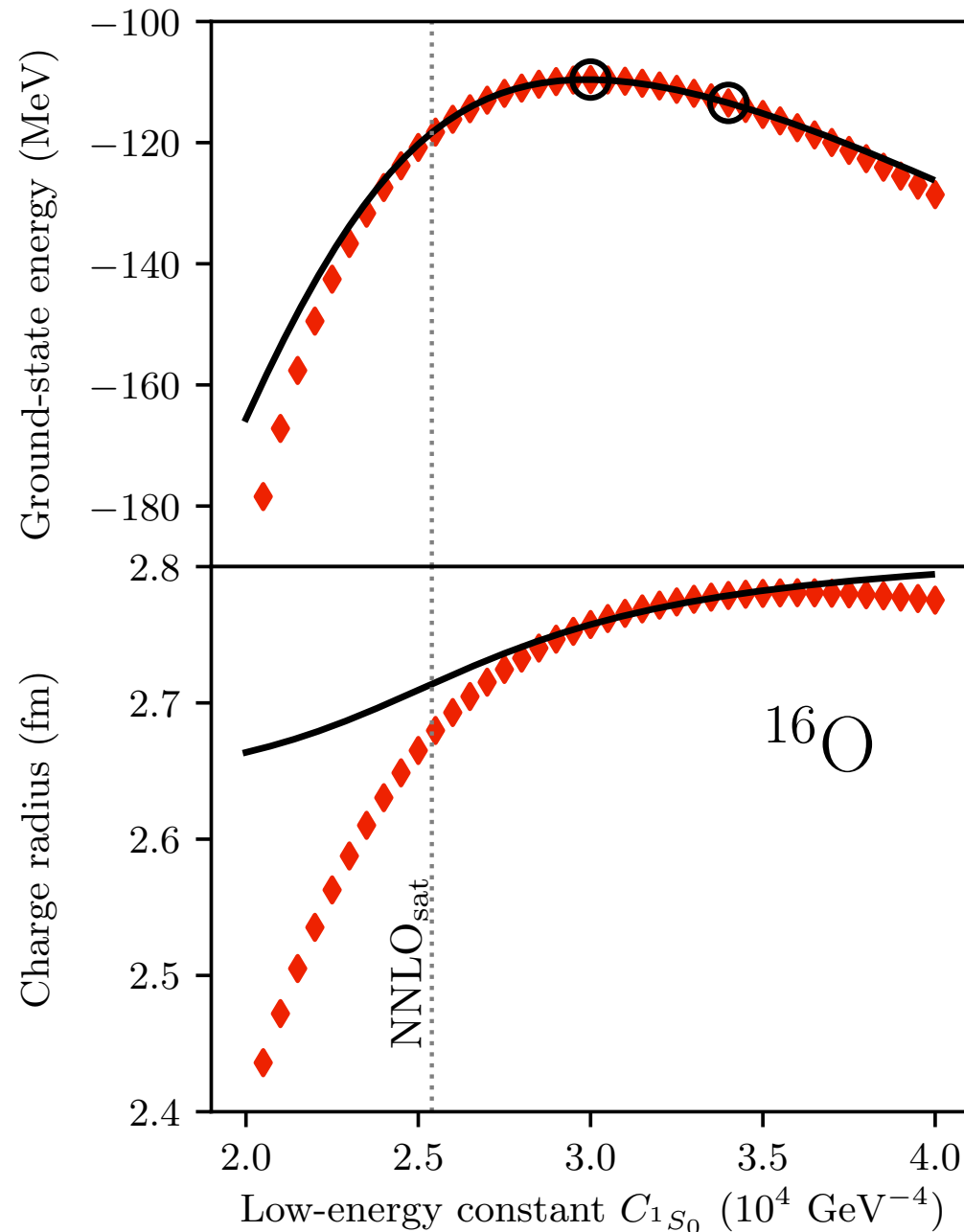


Exact coupled cluster calculations at the singles and doubles level

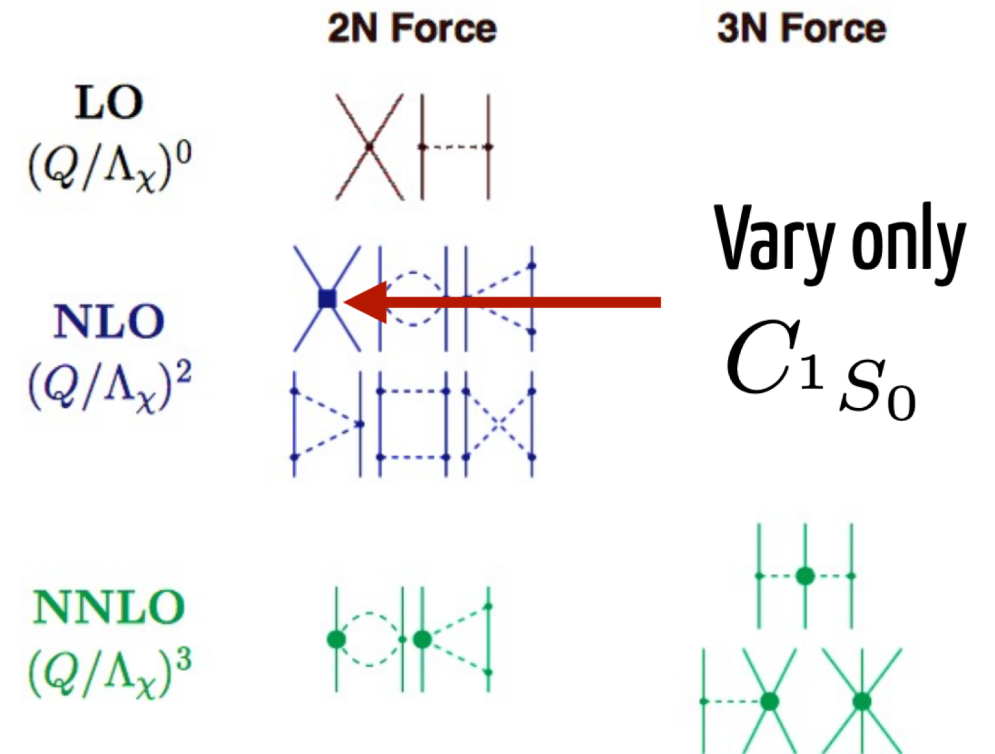


Emulating ab-initio coupled-cluster calculations

Andreas Ekström, Gaute Hagen PRL **123**, 252501 (2019)

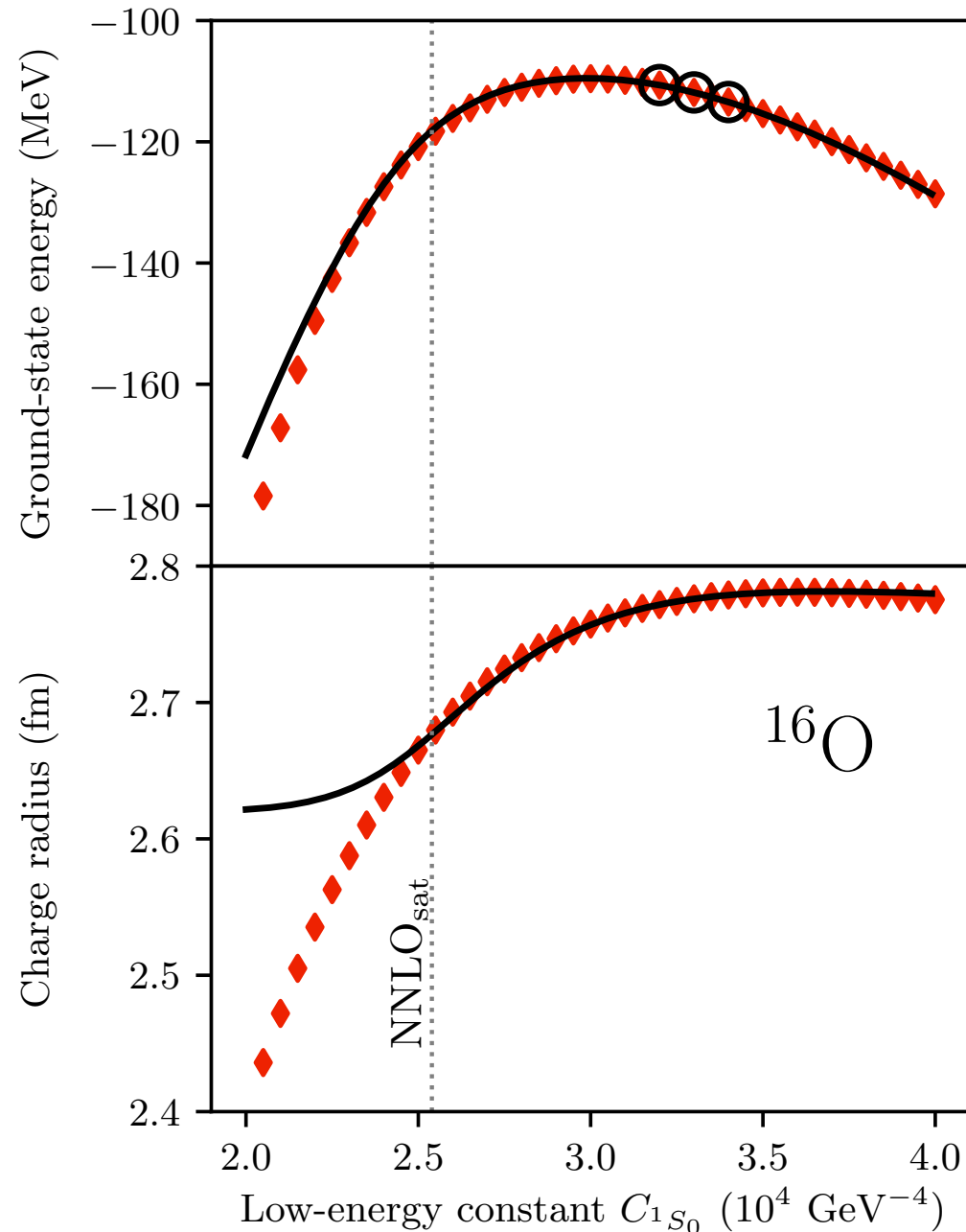


Exact coupled cluster calculations at the singles and doubles level

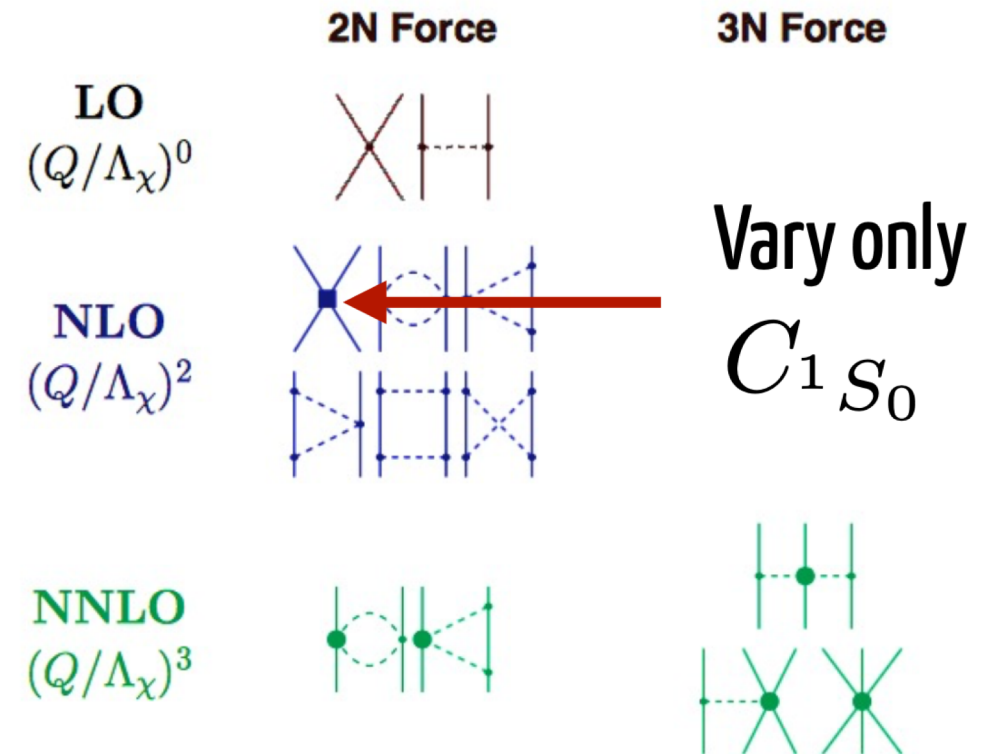


Emulating ab-initio coupled-cluster calculations

Andreas Ekström, Gaute Hagen PRL **123**, 252501 (2019)

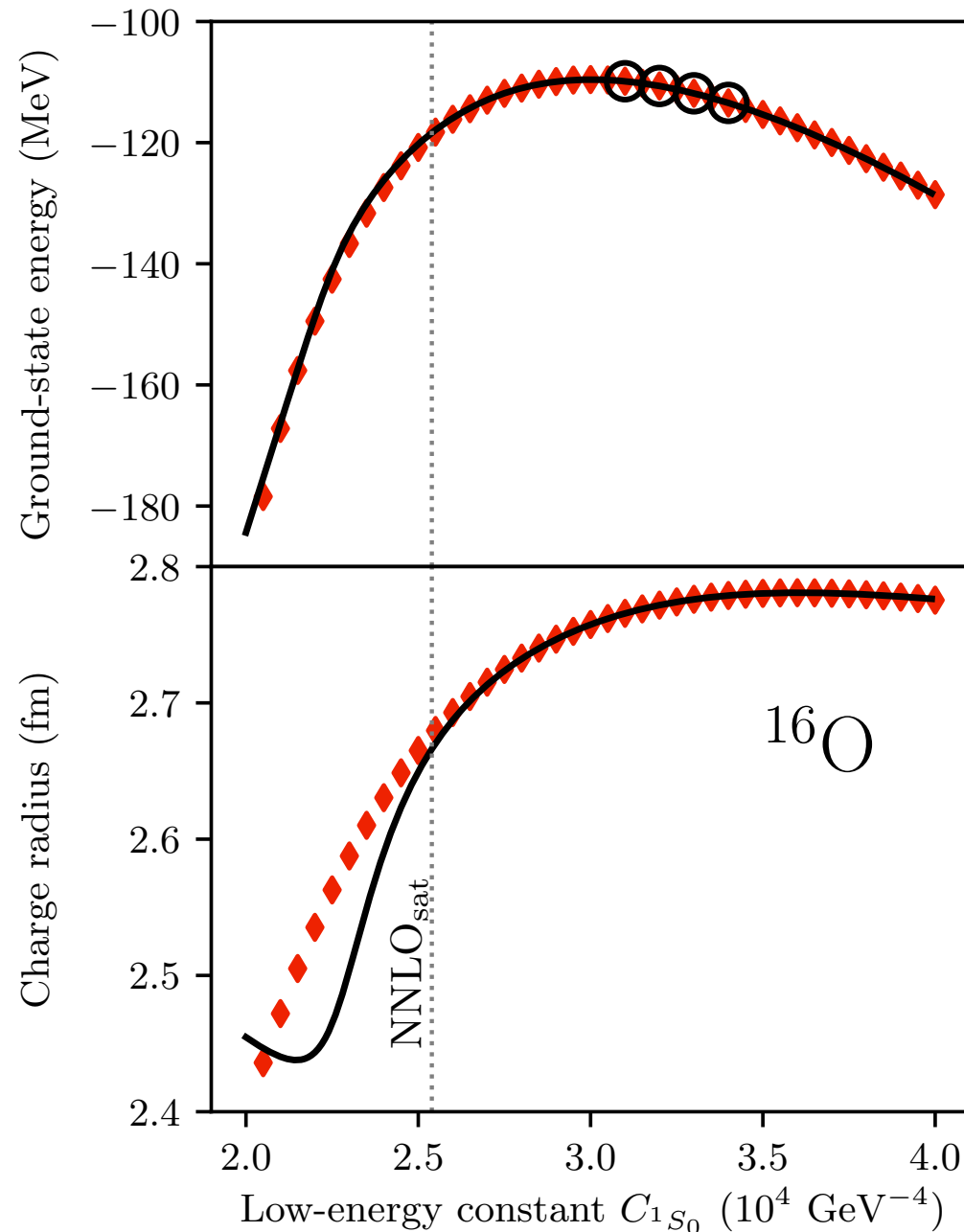


Exact coupled cluster calculations at the singles and doubles level

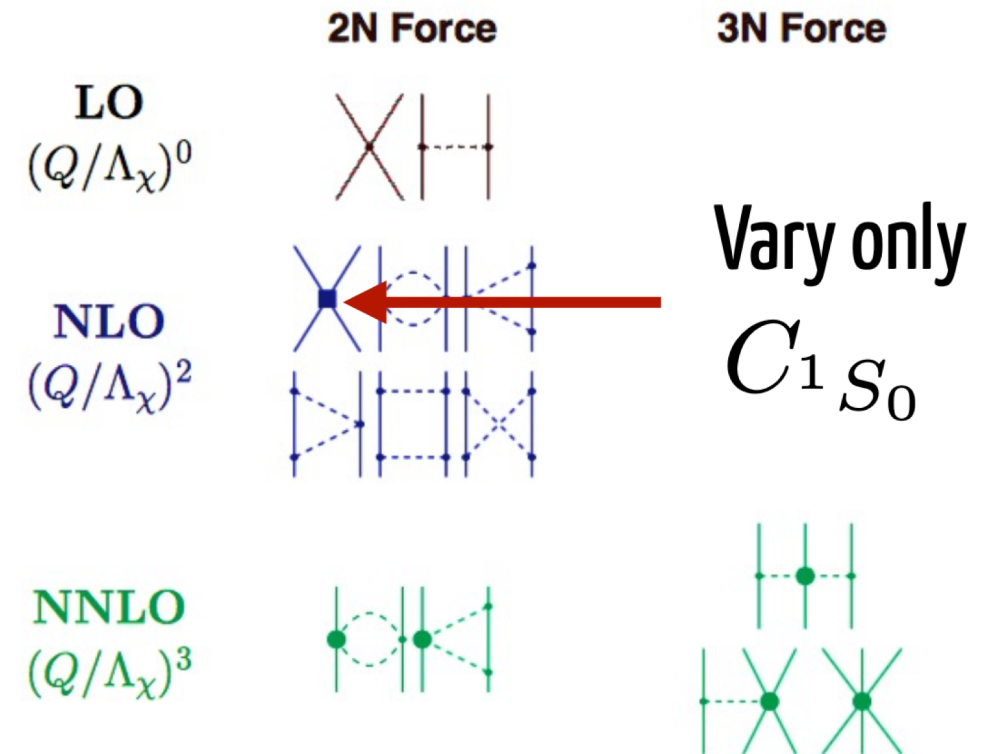


Emulating ab-initio coupled-cluster calculations

Andreas Ekström, Gaute Hagen PRL **123**, 252501 (2019)

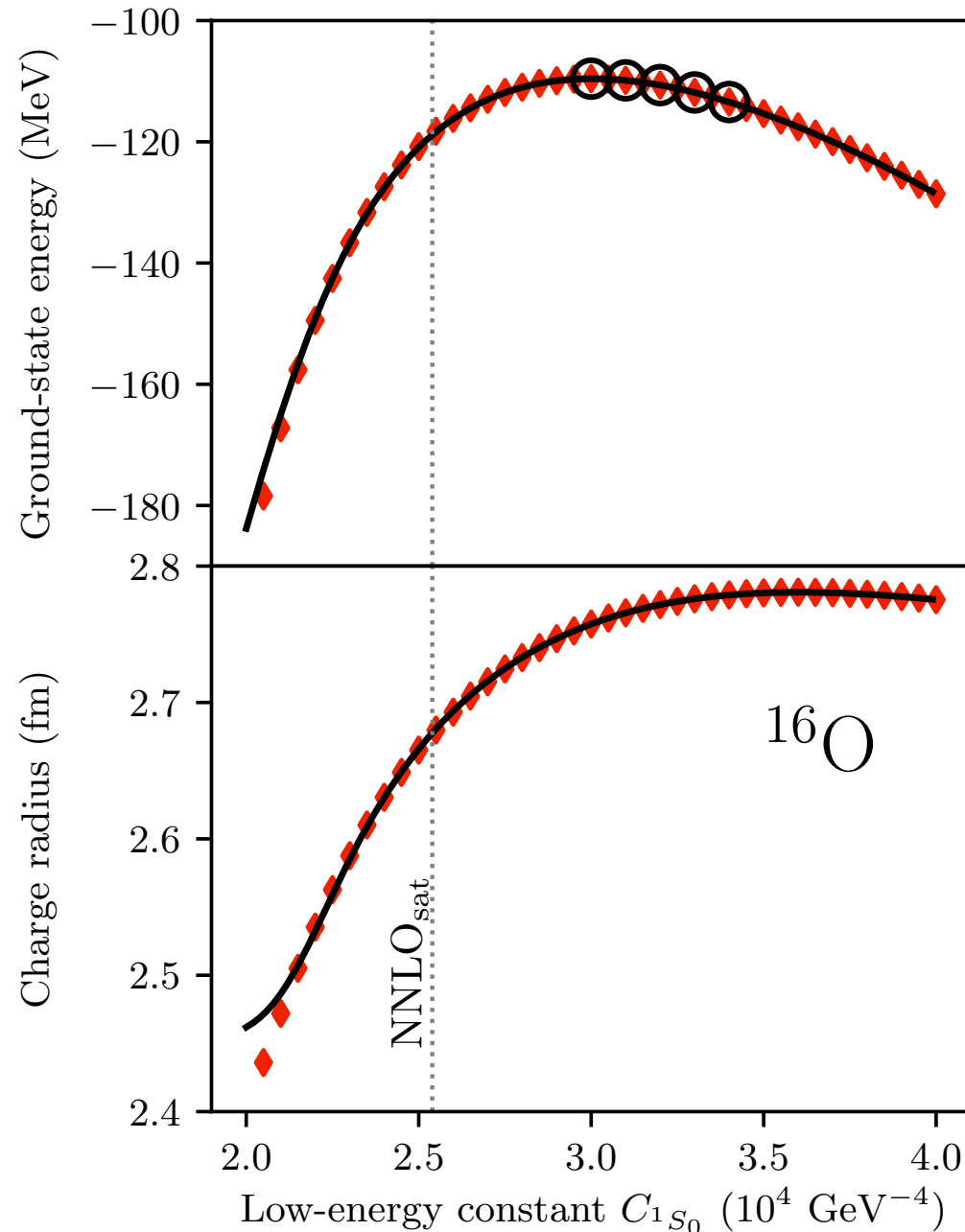


Exact coupled cluster calculations at the singles and doubles level

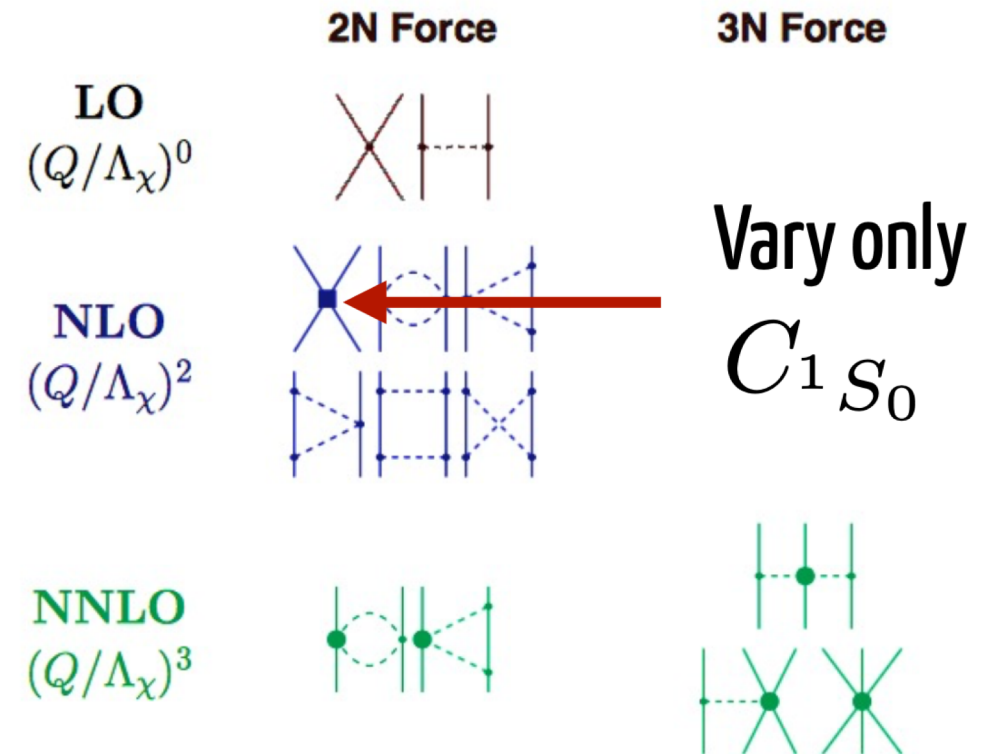


Emulating ab-initio coupled-cluster calculations

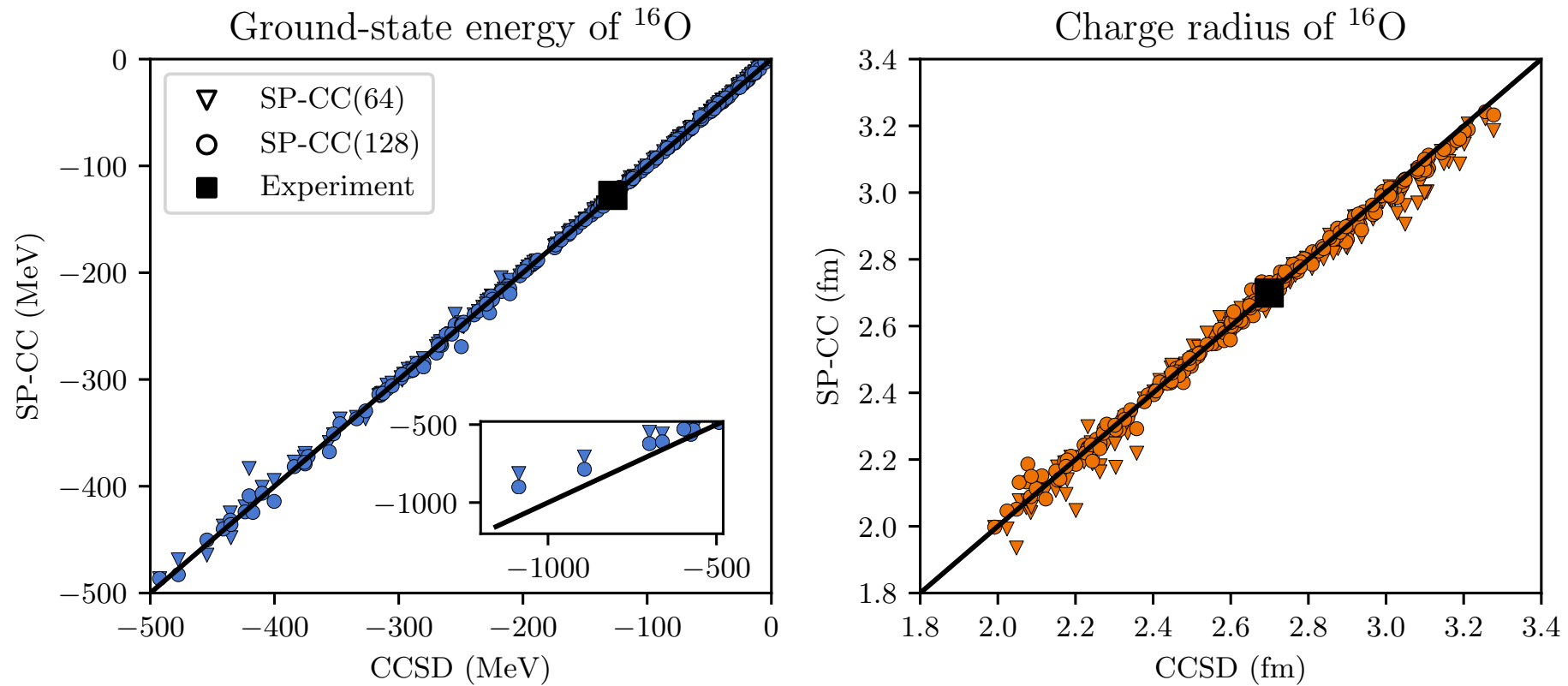
Andreas Ekström, Gaute Hagen PRL **123**, 252501 (2019)



Exact coupled cluster calculations at the singles and doubles level

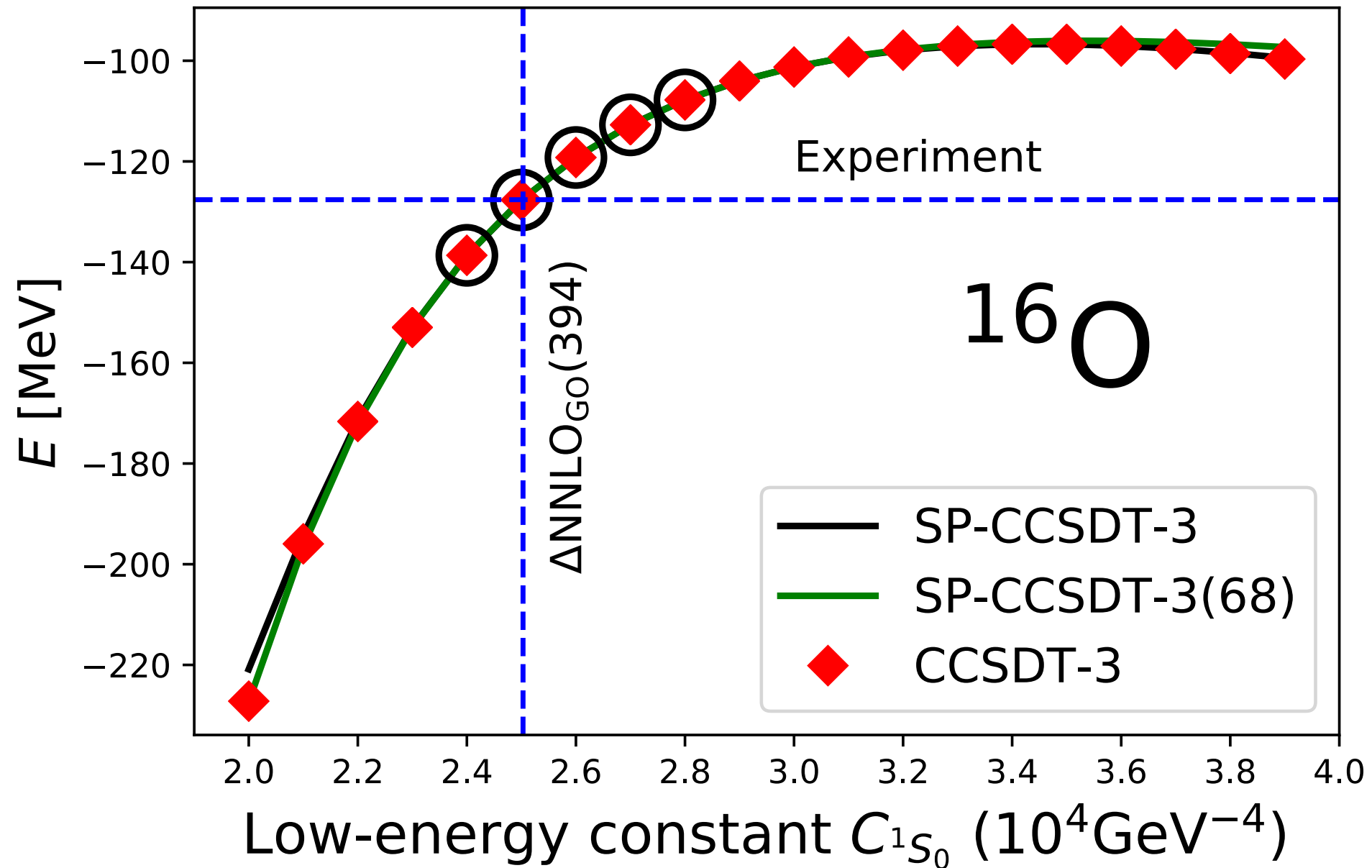


Sub-space projected coupled-cluster – cross validation in 16 dimensions

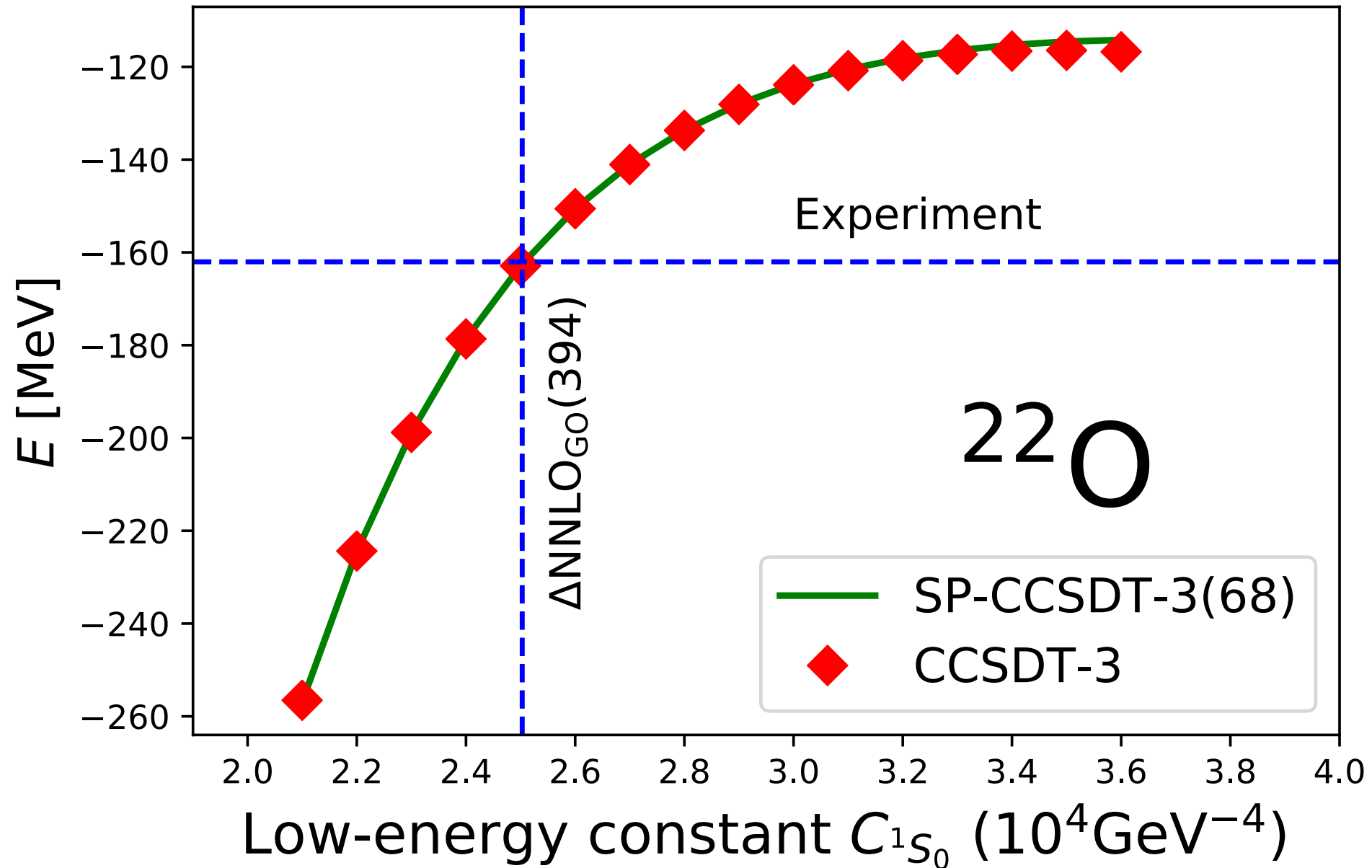


- Select 64 and 128 sub-space vectors in the 16 dimensional space of LECs using a space-filling latin hypercube design
- Select 200 randomly exact CCSD calculations in a 20% domain around NNLO_{sat}
- With 64 subspace vectors we achieve a 1% accuracy relative to exact CCSD solutions

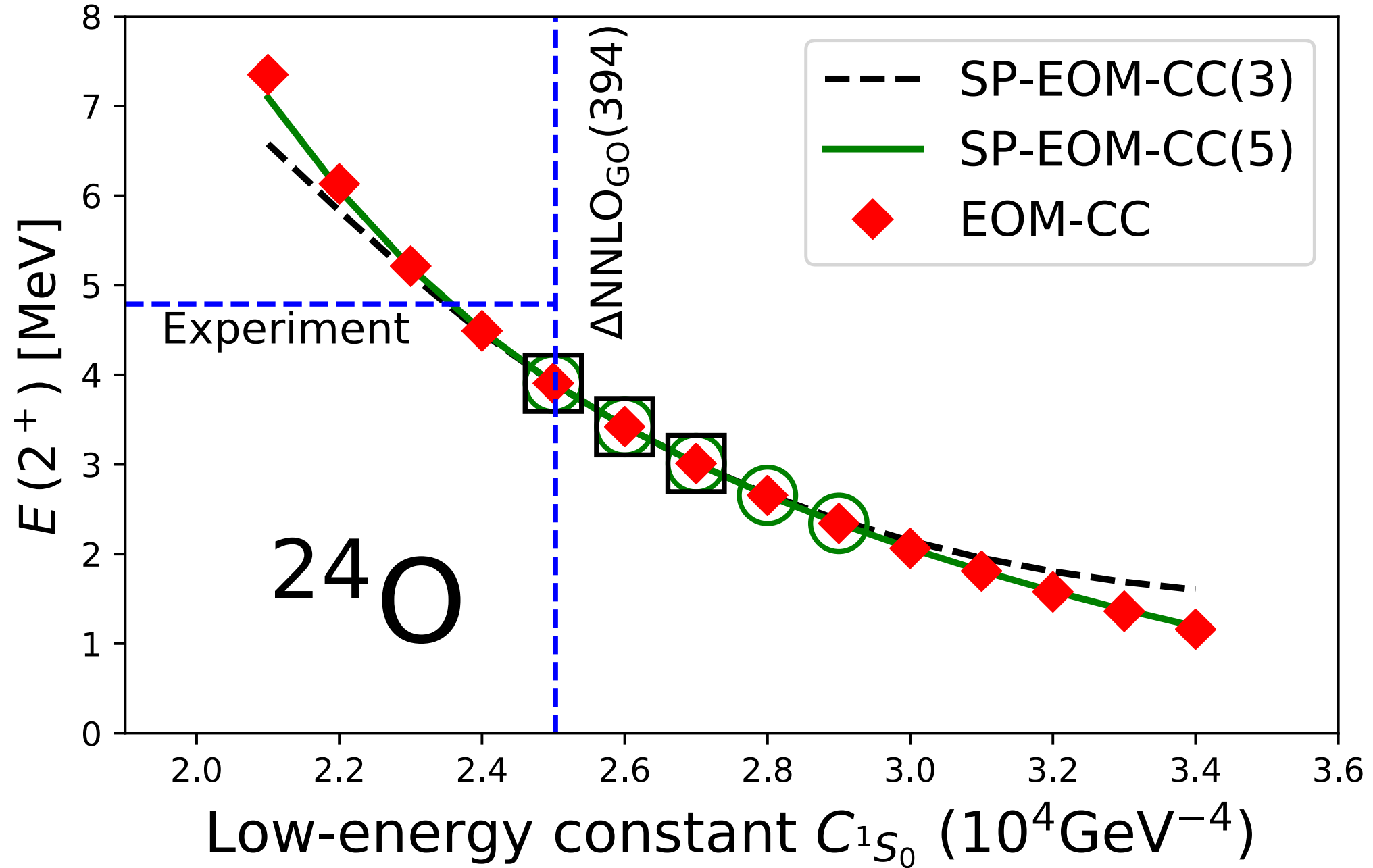
SPCC with triples excitations



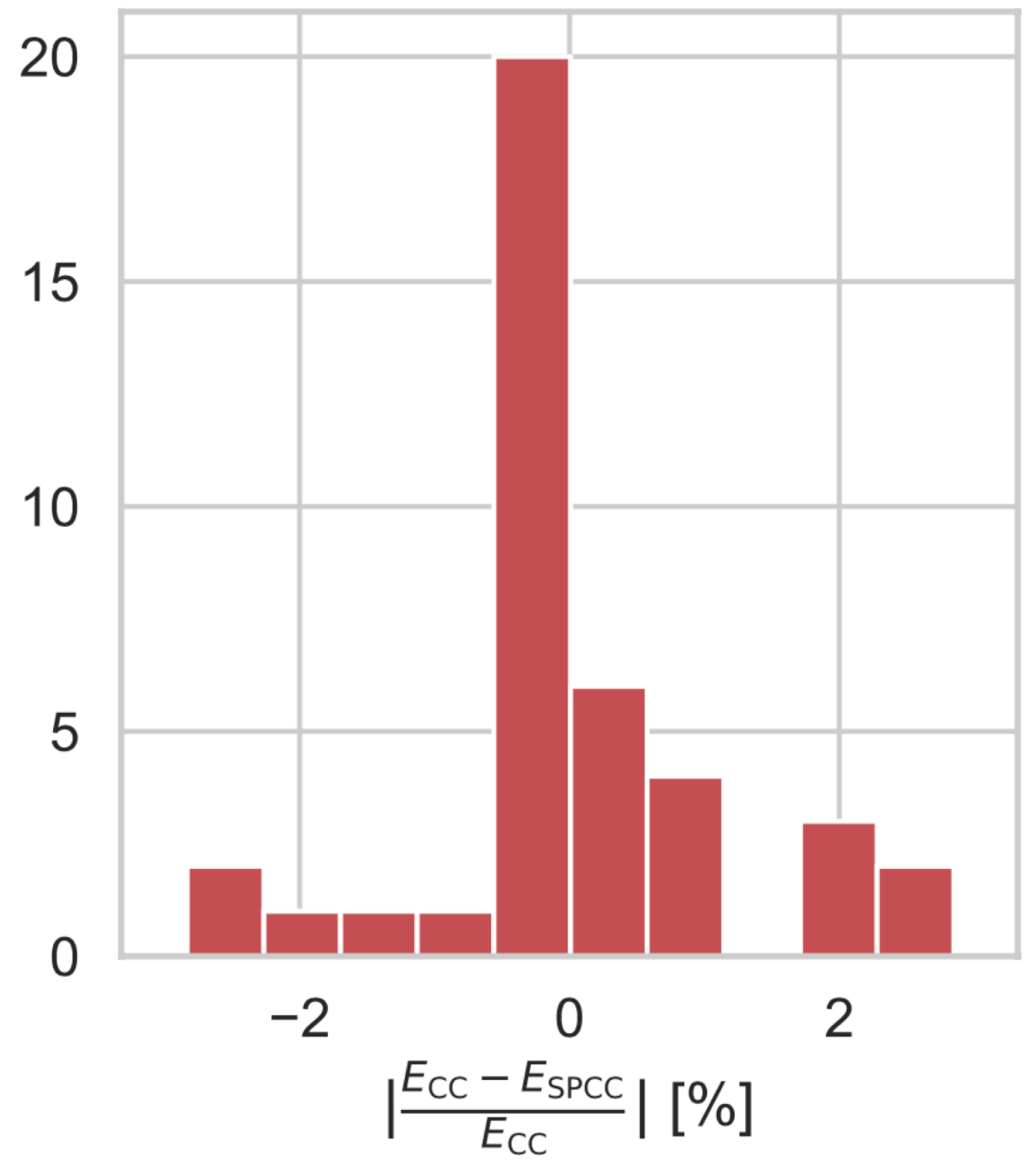
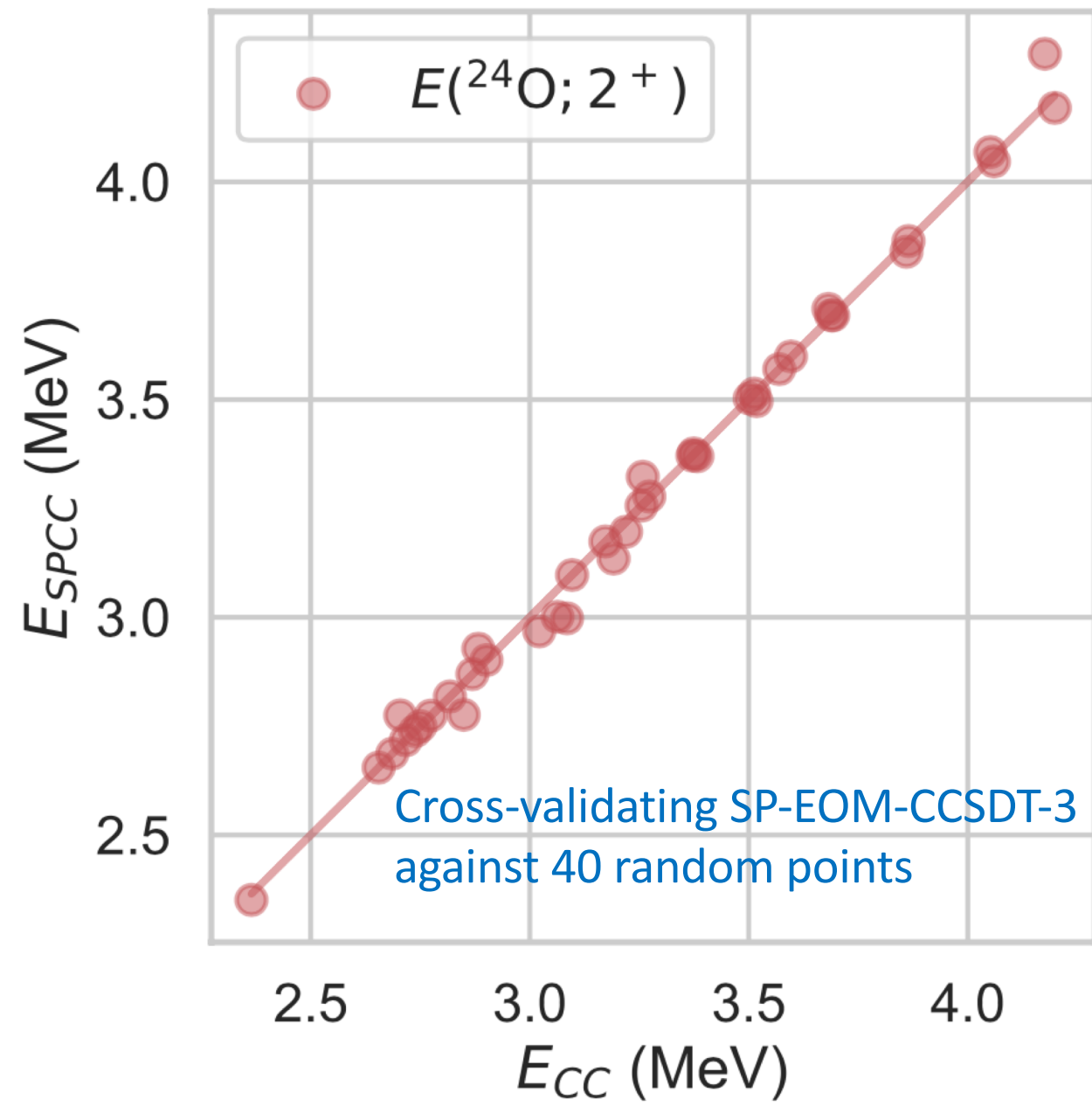
SPCC with triples excitations



SPCC for excited states



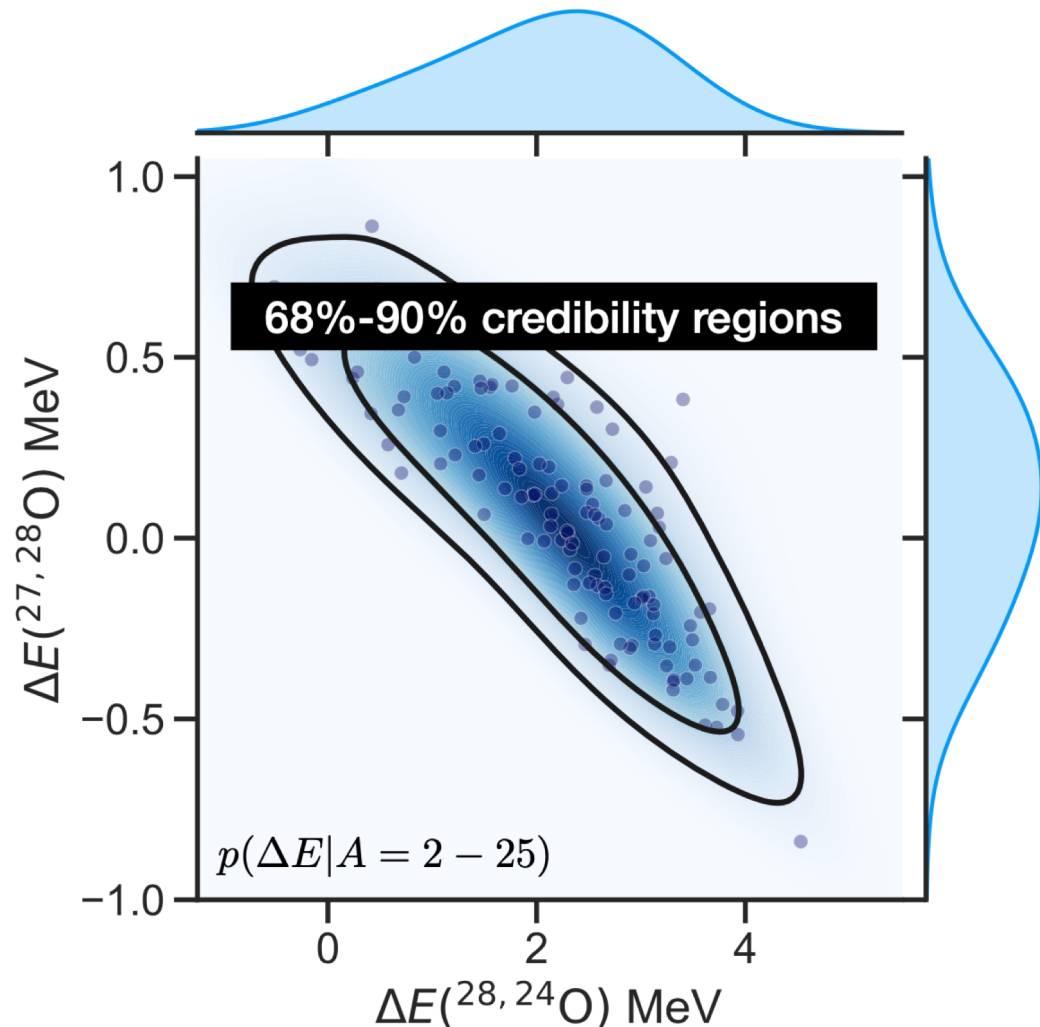
SPCC for excited states



Do chiral Hamiltonians predict a bound ^{28}O ?

Ekström, Forssén, Hagen, Jiang, Papenbrock, Sun, Vernon

We claim with 98% certainty that ^{28}O is unbound

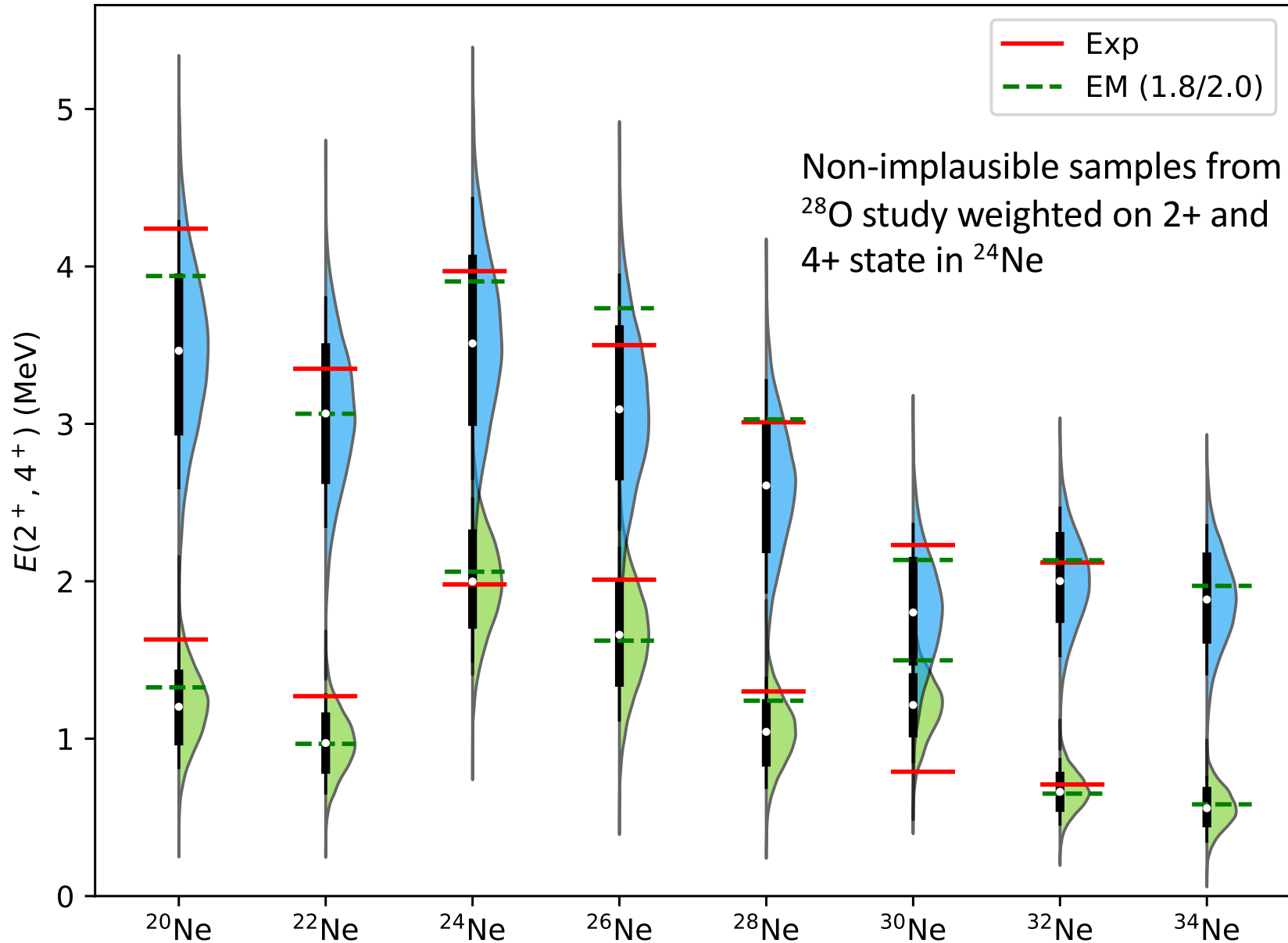


- Used history matching and emulators and performed 10^8 predictions for ground- and excited states of nuclei up to ^{24}O
- Sample the parameter posterior using MCMC
- We update the parameter posterior with information from oxygen-25 and subsequently draw 121 parameter samples used in our prediction of oxygen-27/28
- Oxygen-28 prediction is sensitive to small changes in the parameters
- It turns out the weighting on ^{25}O has little impact on rotational structure in neon isotopes

Prediction for ^{28}O shown as probability distribution where solid lines indicate the 68% and 90% probability density regions

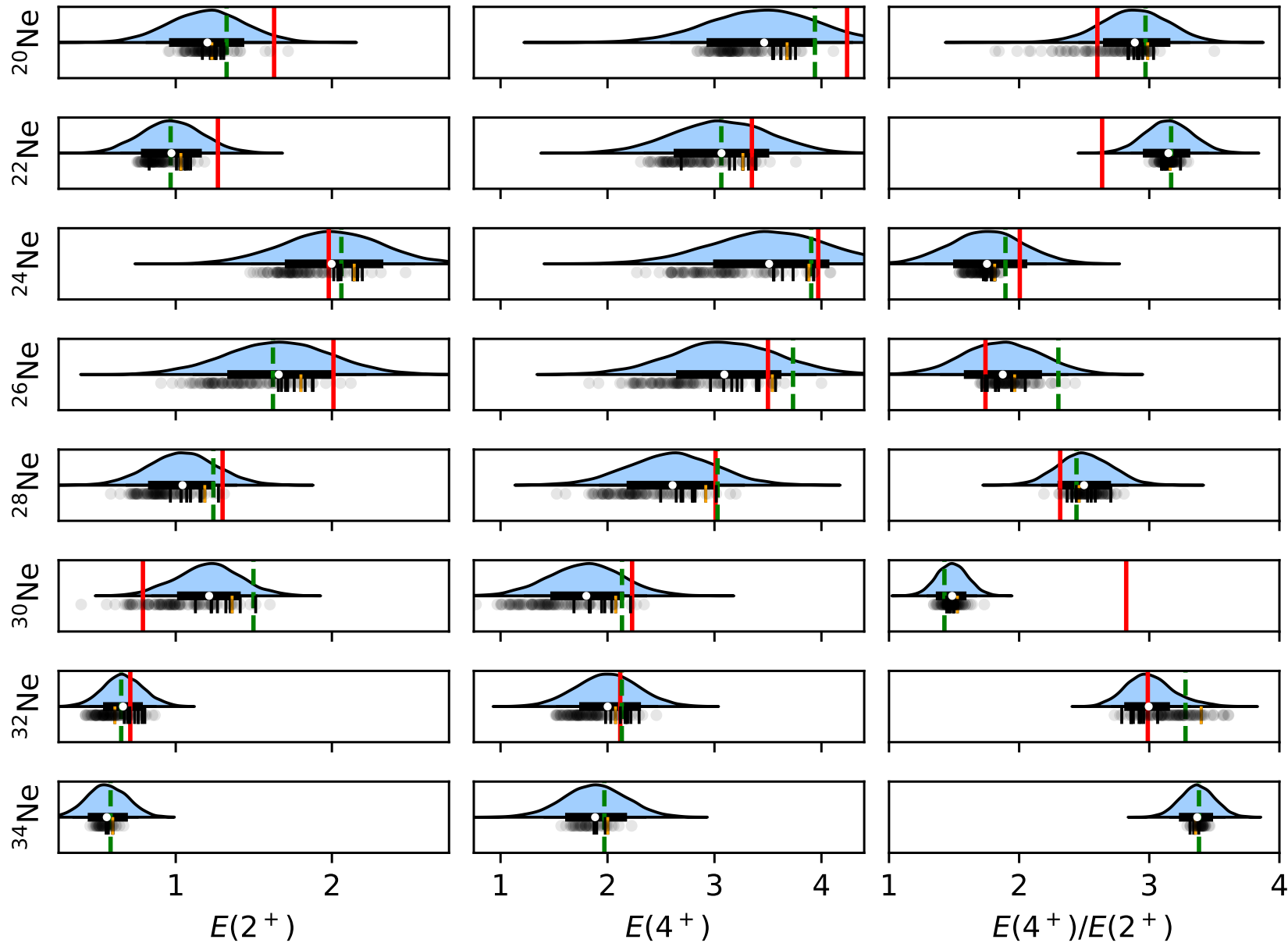
Also see Christian Forssen's talk

Rotational structure of neon isotopes with chiral interactions at NNLO



- Posterior predictive distributions for the 2^+ and 4^+ states in neon
- Spectra generally too compressed
- Rotational structure of ^{32}Ne in good agreement with data
- We predict that ^{34}Ne is as rotational as ^{32}Ne and ^{34}Mg

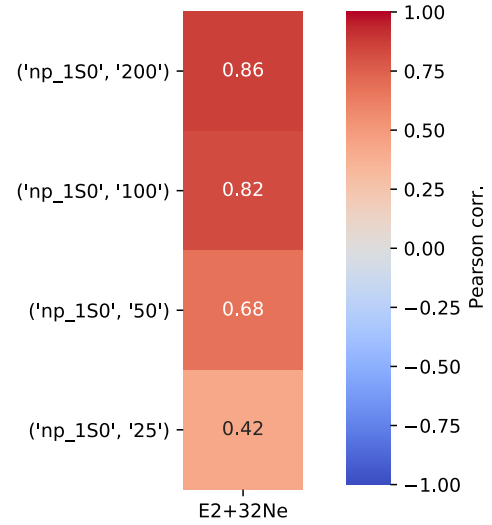
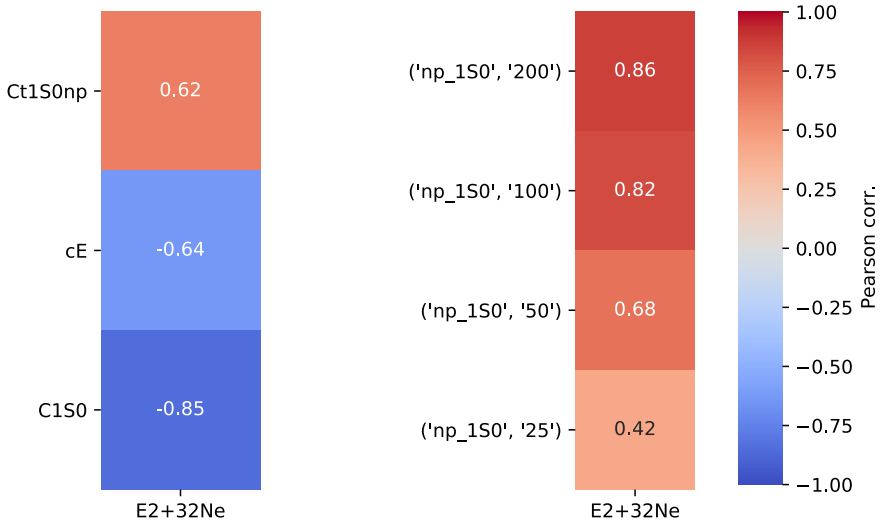
Rotational structure of neon isotopes with chiral interactions at NNLO



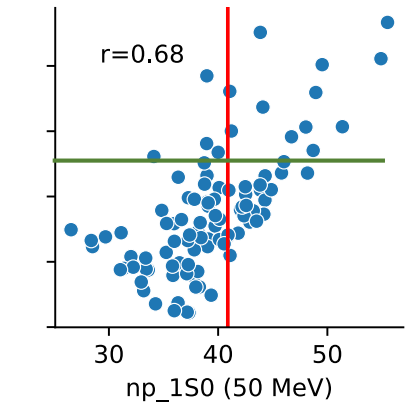
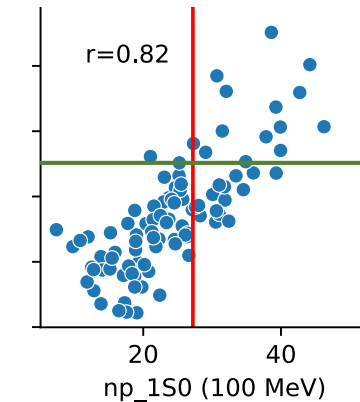
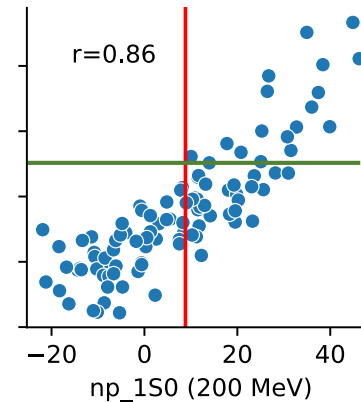
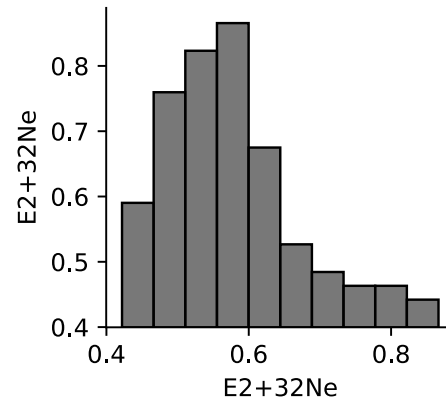
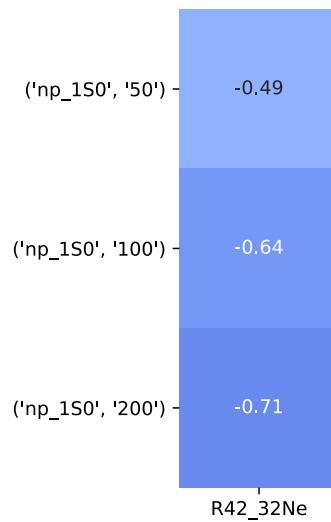
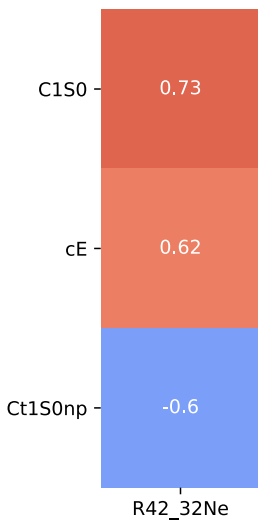
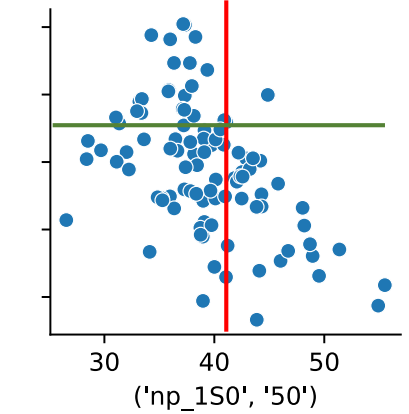
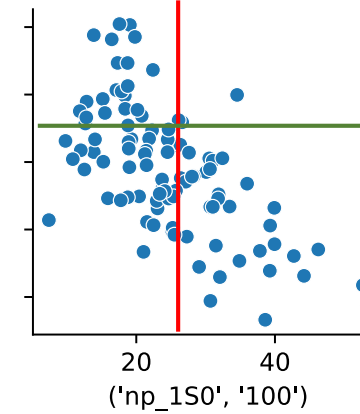
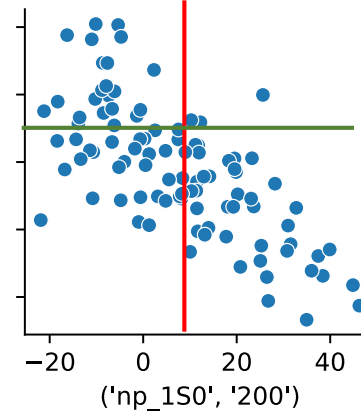
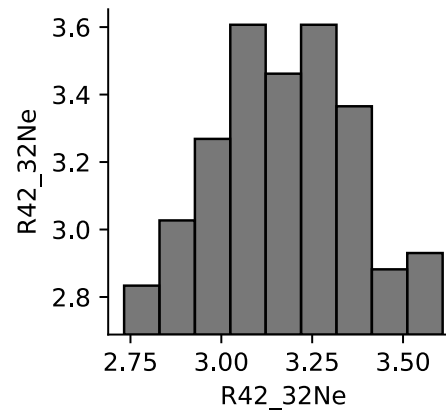
- Posterior predictive distributions for the 2^+ and 4^+ states in neon
- Spectra generally too compressed
- Rotational structure of ^{32}Ne in good agreement with data
- We predict that ^{34}Ne is as rotational as ^{32}Ne and ^{34}Mg

What drives deformation in ^{32}Ne ?

Pearson correlation coefficient

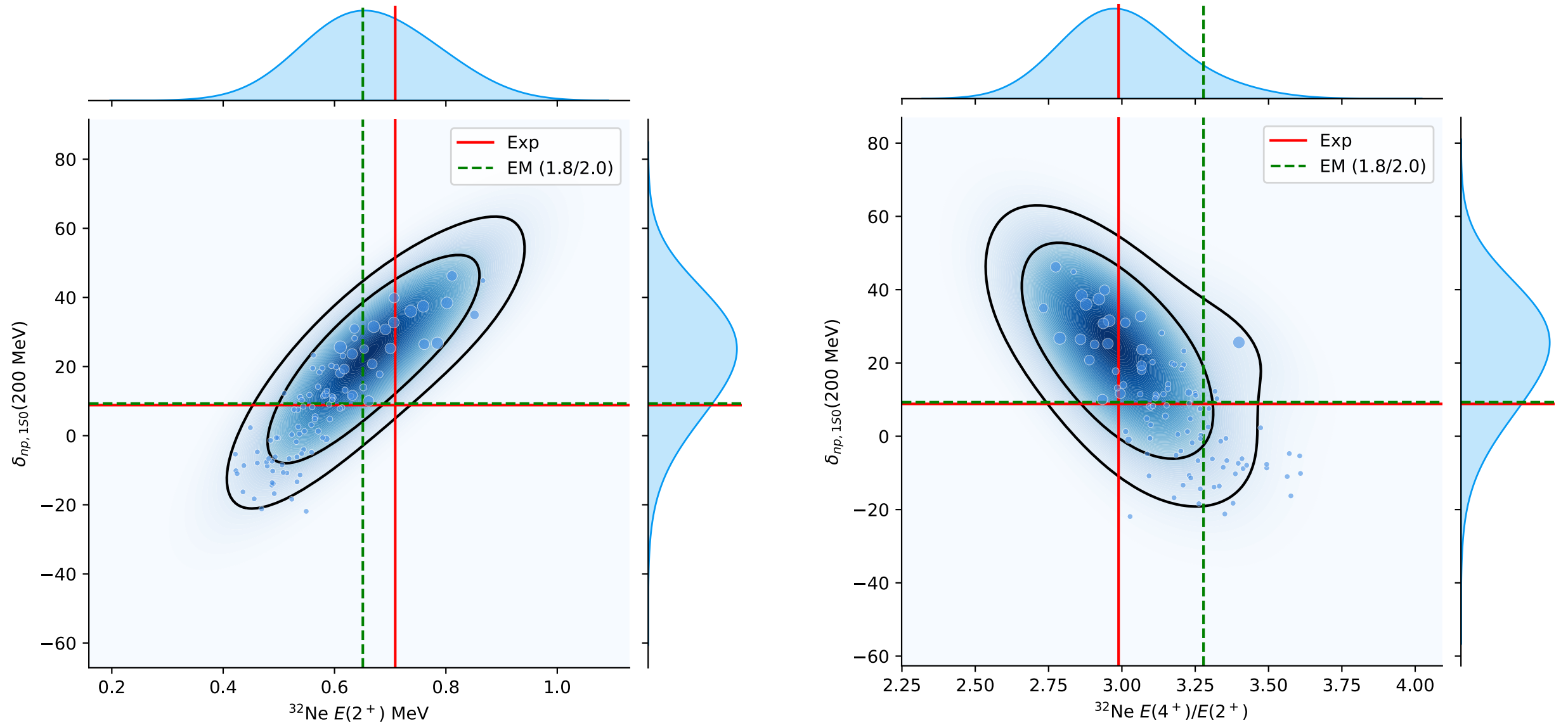


Results from coupled-cluster computations with angular momentum projection; based on ensemble of non-implausible Hamiltonians that predict structure of 280



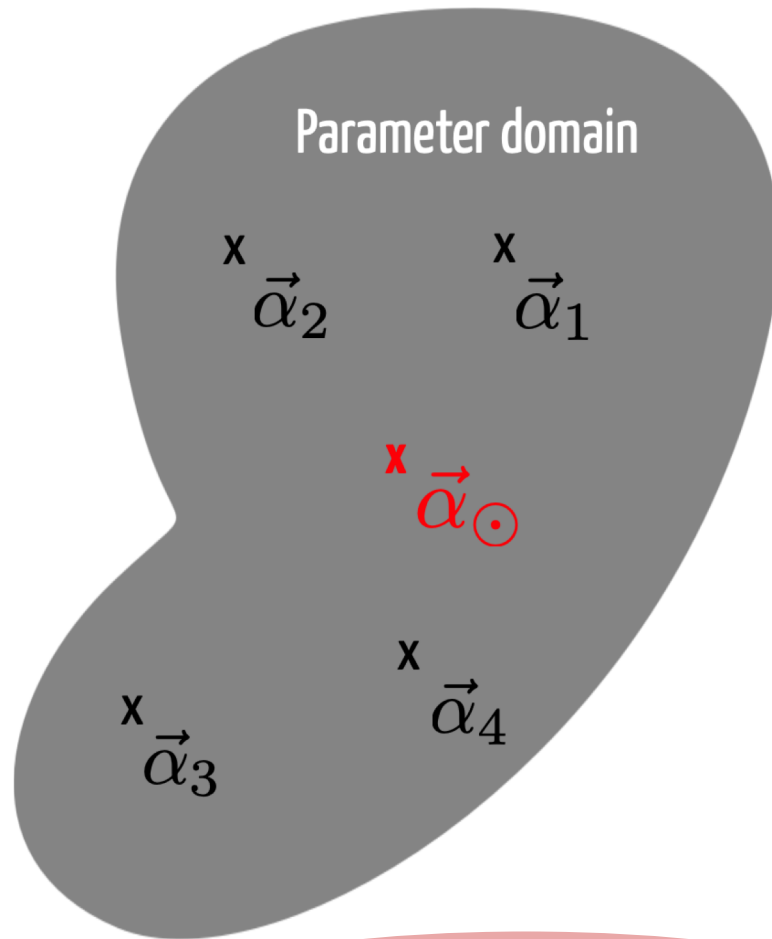
What drives deformation in ^{32}Ne ?

Non-implausible samples from ^{28}O study weighted on 2+ and 4+ state in ^{24}Ne



Joint posterior predictive distributions. Solid lines indicate the 68% and 90% probability density regions

Linking deformation to microscopic nuclear forces using emulators



- Eigenvector continuation method [Frame D. et al., Phys. Rev. Lett. 121, 032501 (2018), S. König et al Phys. Lett. B 810 (2020) 135814]

- Write the Hamiltonian in a linearized form

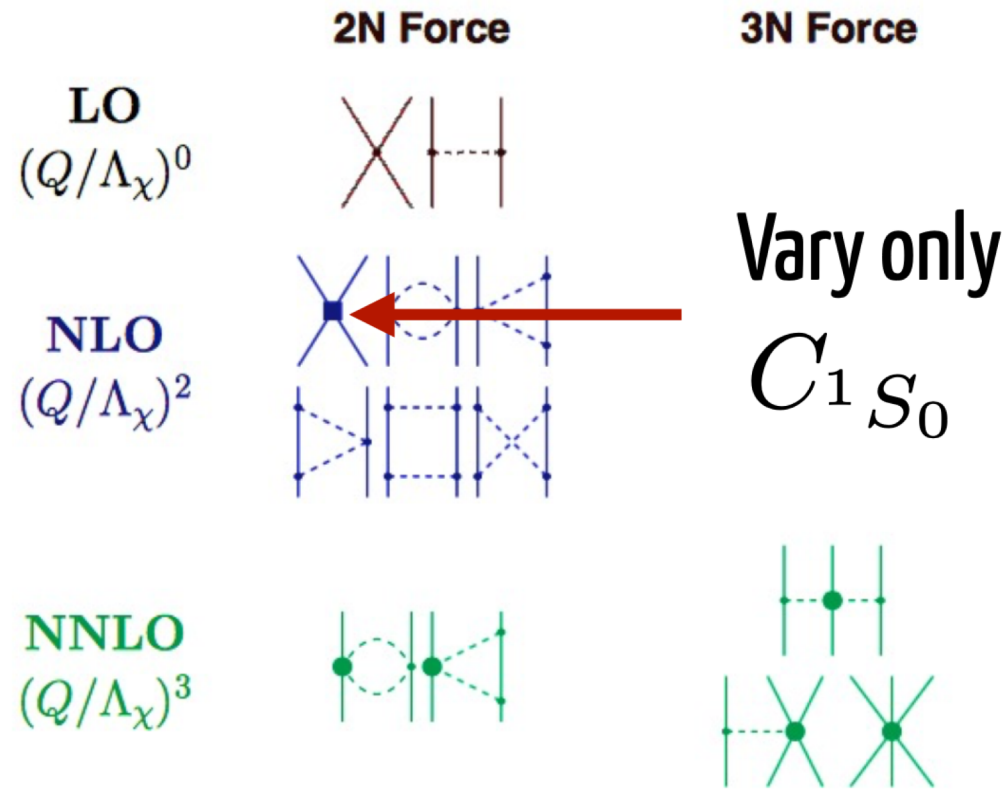
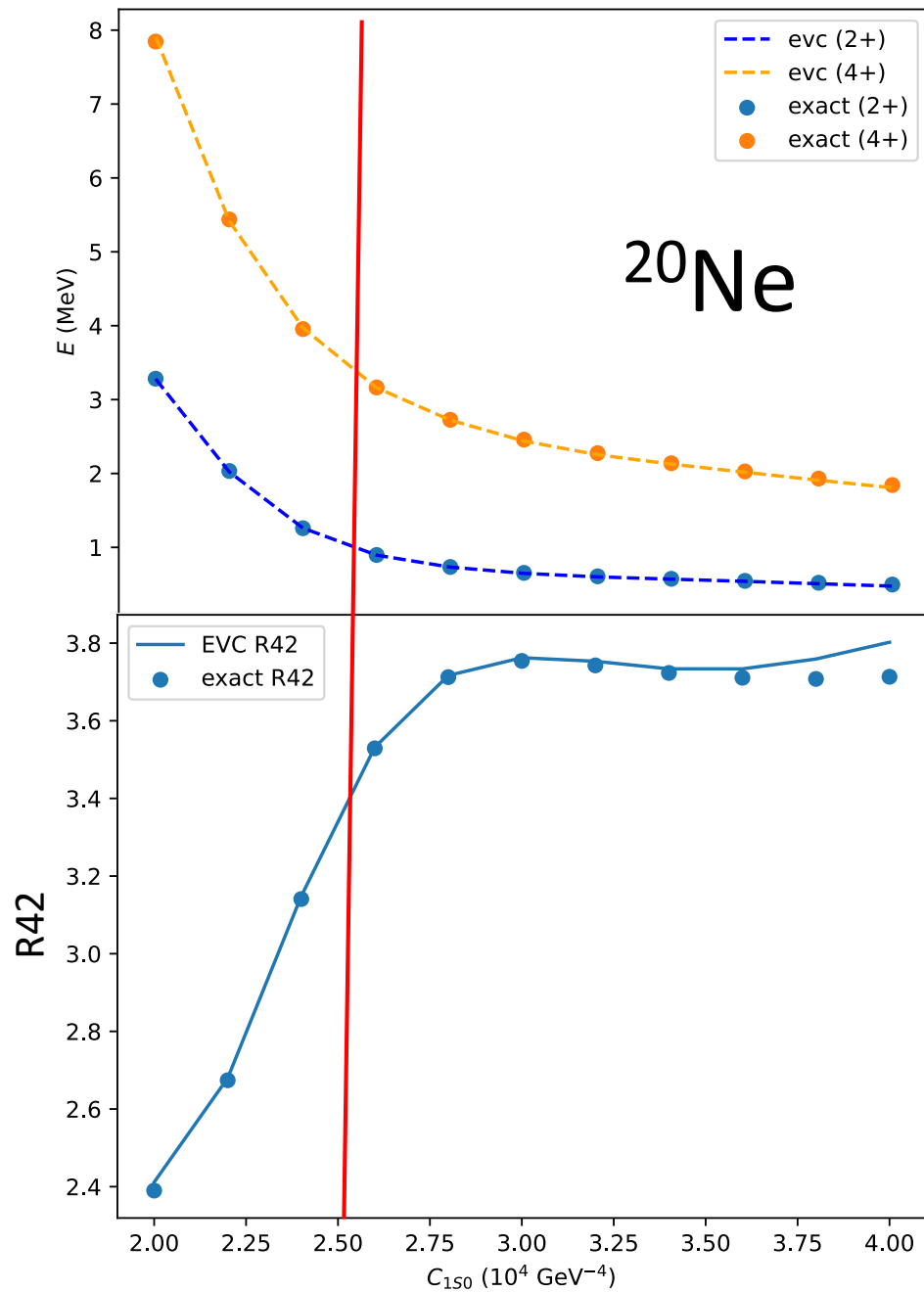
$$H(\vec{\alpha}) = h_0 + \sum_{i=1}^{N_{\text{LECS}}=17} \alpha_i h_i$$

- Select “training points” where we solve exact problem
- Project a target Hamiltonian onto subspace of training vectors and diagonalize the generalized eigenvalue problem

$$E^{(J)} = \frac{\langle \Phi(\alpha_{\odot}) | P_J H | \Phi(\alpha_{\odot}) \rangle}{\langle \Phi(\alpha_{\odot}) | P_J | \Phi(\alpha_{\odot}) \rangle}$$

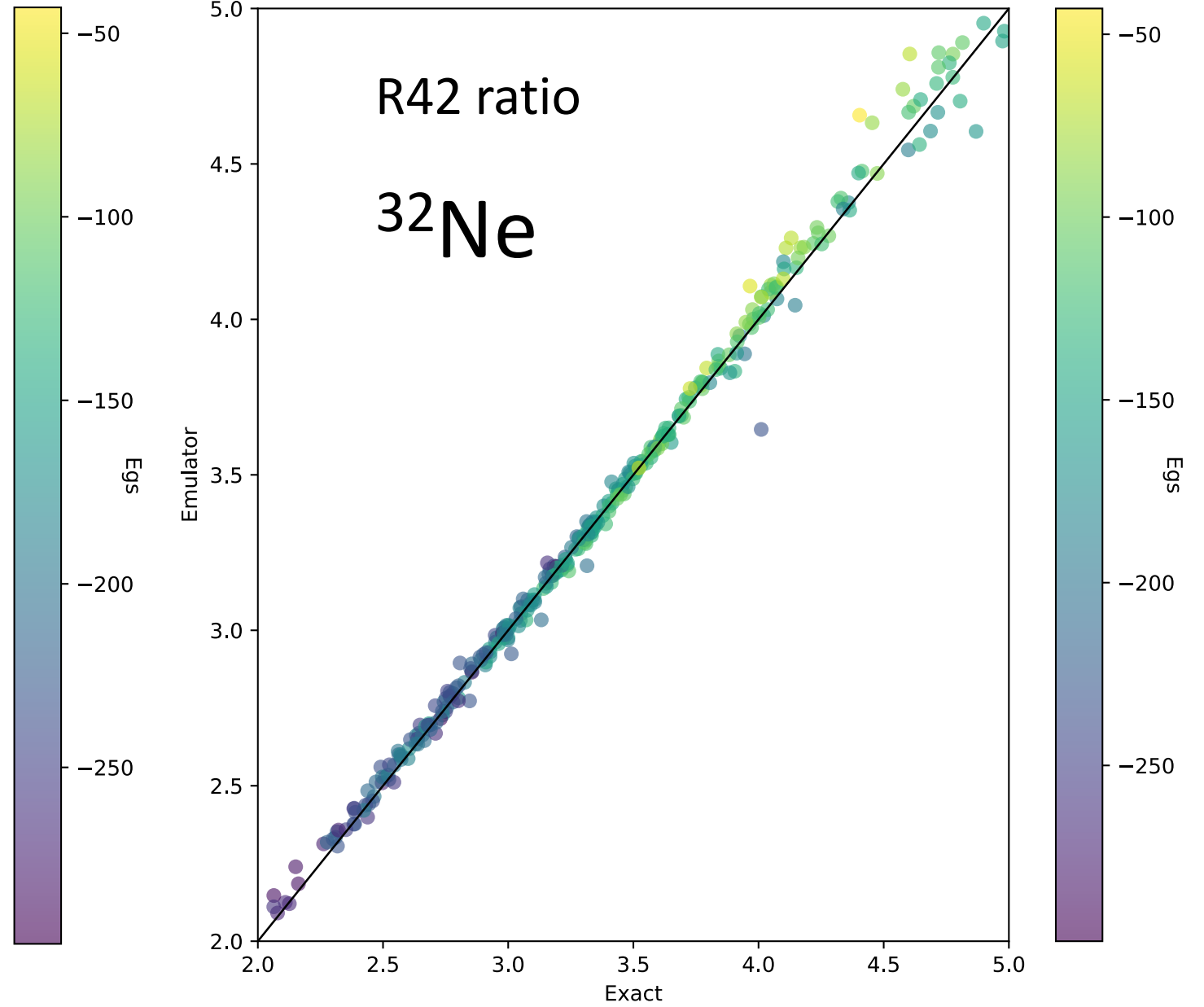
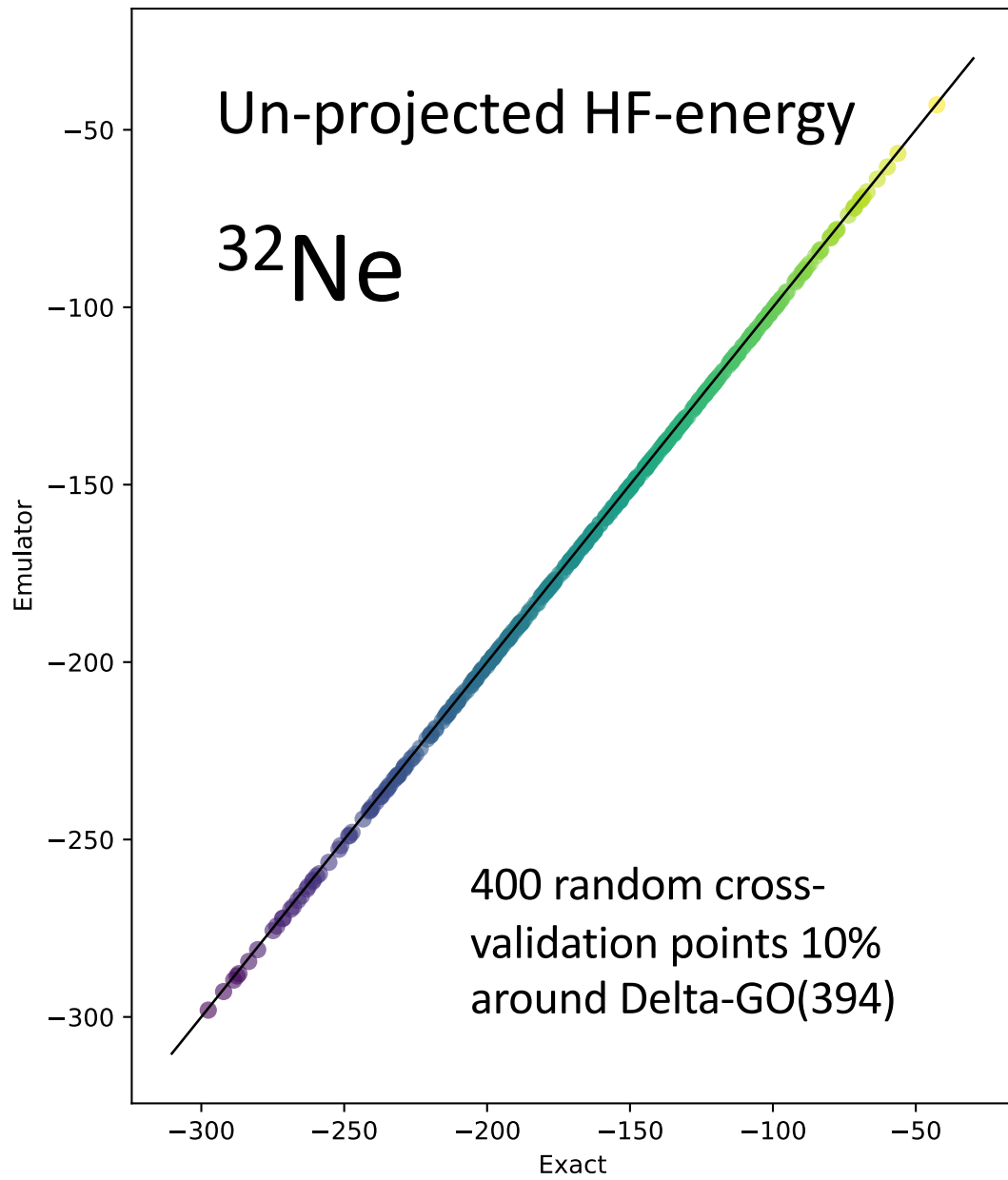
$$\mathbf{H}(\vec{\alpha}_{\odot}) \vec{c} = E(\vec{\alpha}_{\odot}) \mathbf{N} \vec{c},$$

Linking deformation to nuclear forces

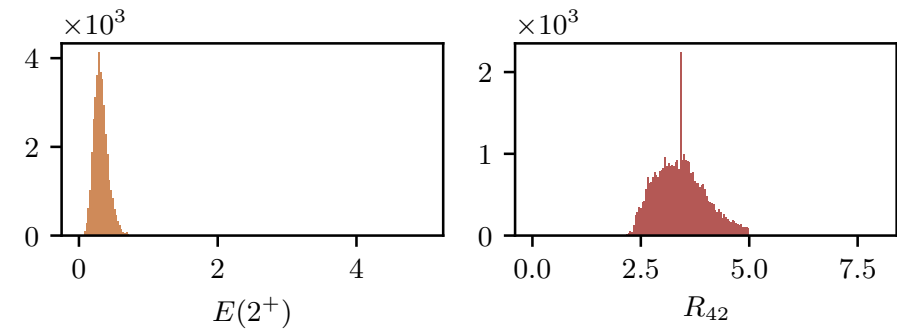
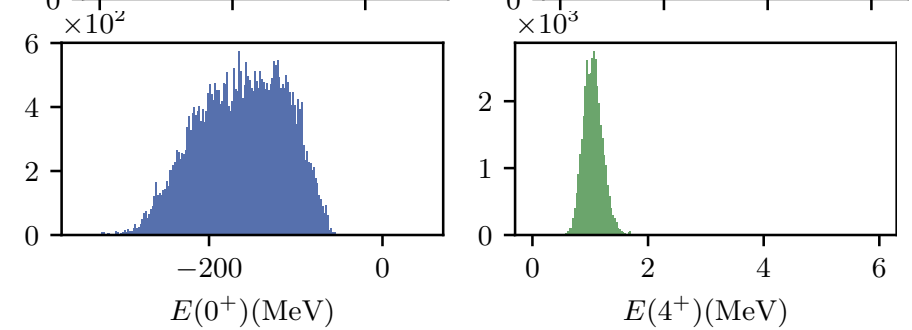
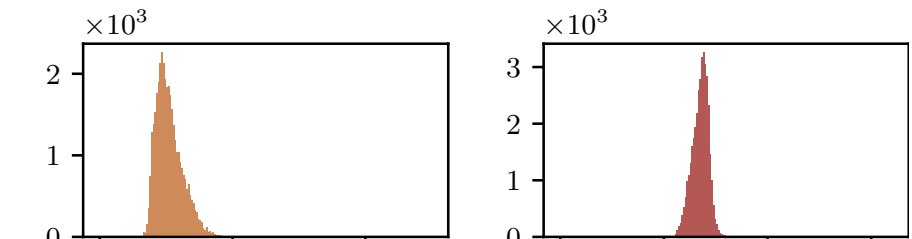
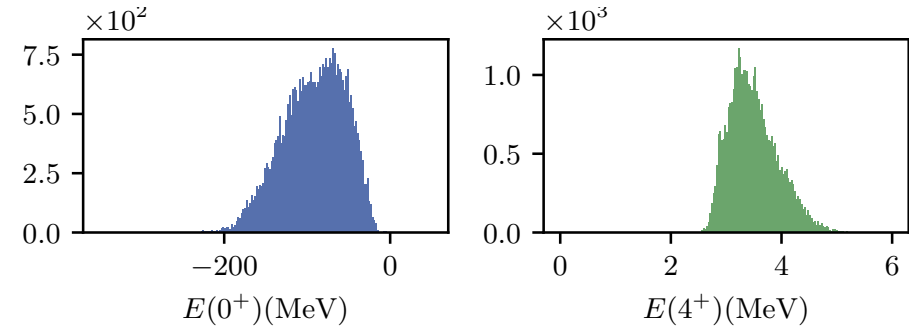
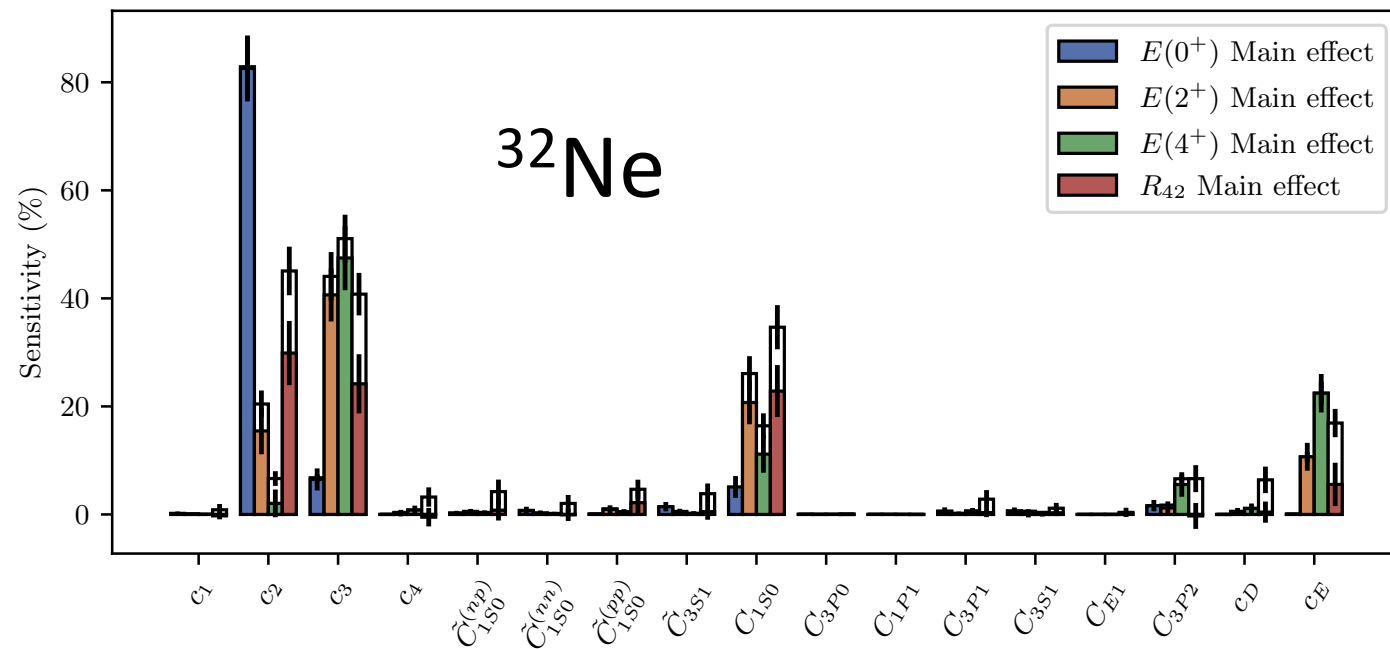
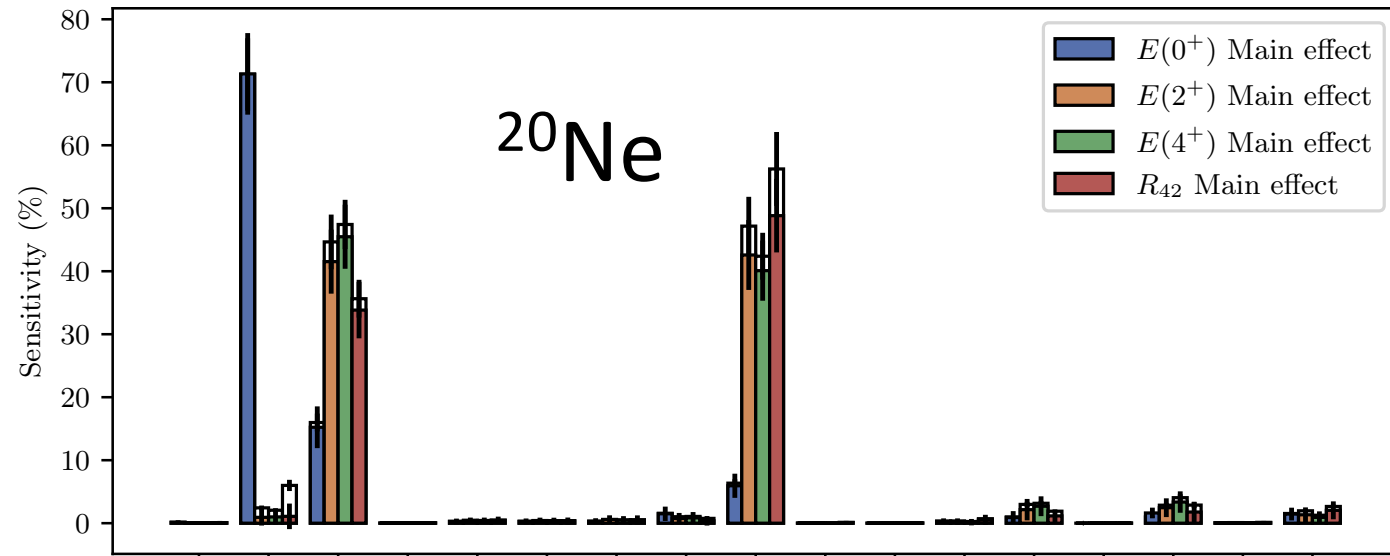


- Constructed accurate and efficient emulator of projected HF using 68 training vectors
- Training points obtained by using Latin Hypercube sampling within 20% of original low-energy constants

Linking deformation to nuclear forces



Linking deformation to nuclear forces



M1 transition in ^{48}Ca

- Large $B(M1: 0^+ \rightarrow 1^+)$ due to strong $\nu 1f_{7/2} \rightarrow \nu 1f_{5/2}$ excitation
- Darmstadt results are consistent with strong quenching factor (0.75) for the isovector strength
- Similarity of 1B operators in spin-flip M1 and GT transitions has been used as explanation for strong quenching. We test this by explicitly including 2B operators.

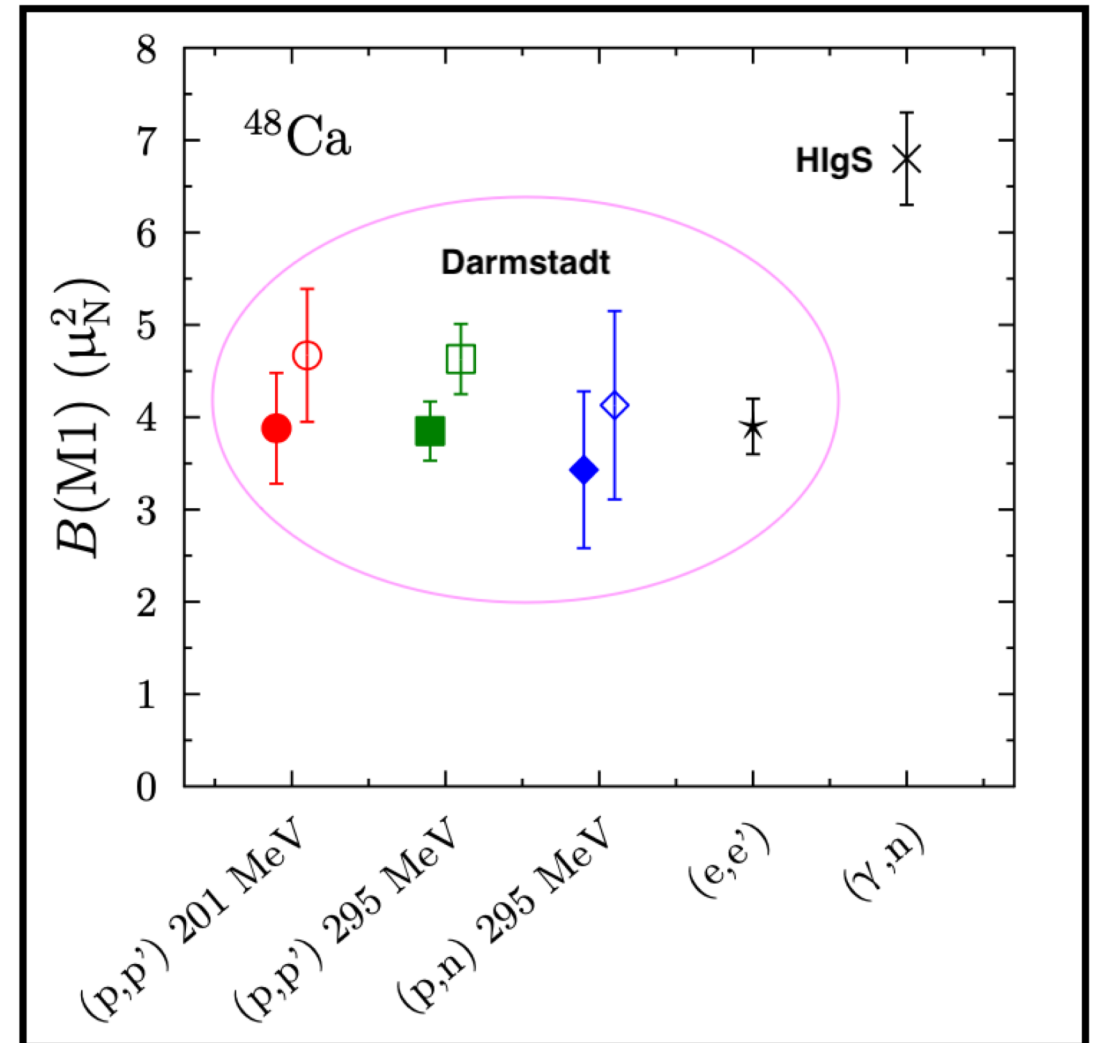


Figure adapted from PRC **93**, 041302(R) (2016)

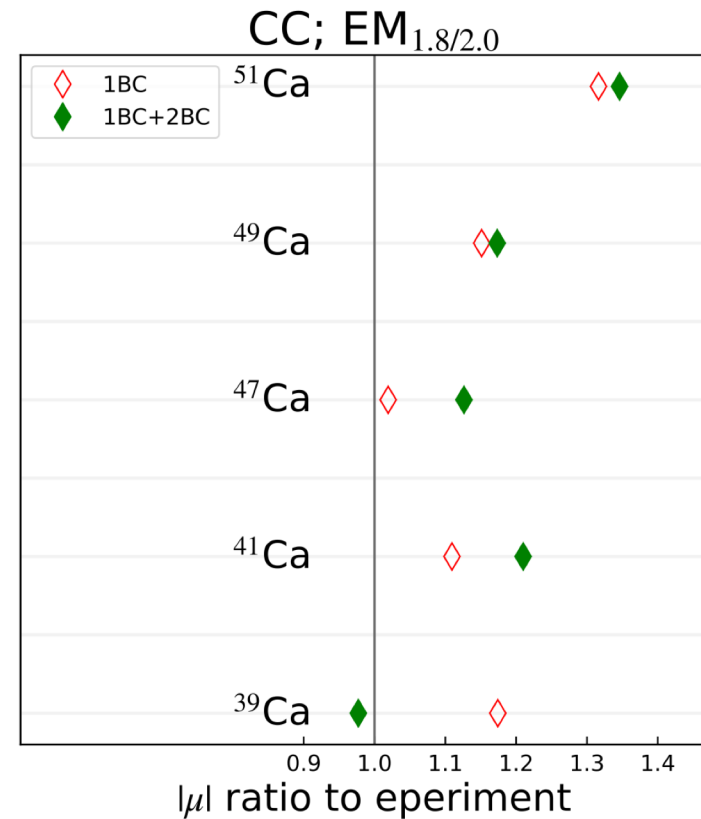
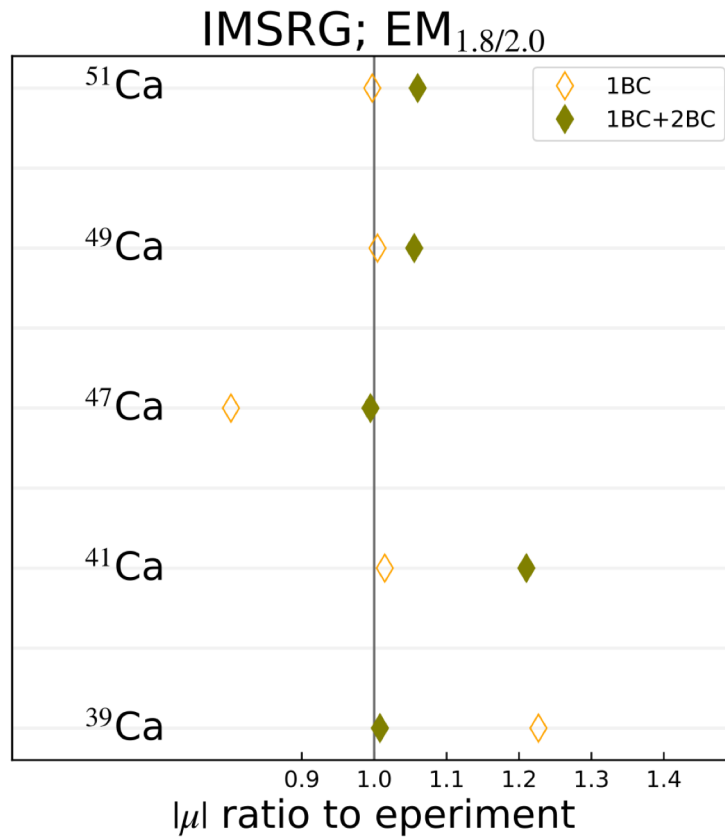
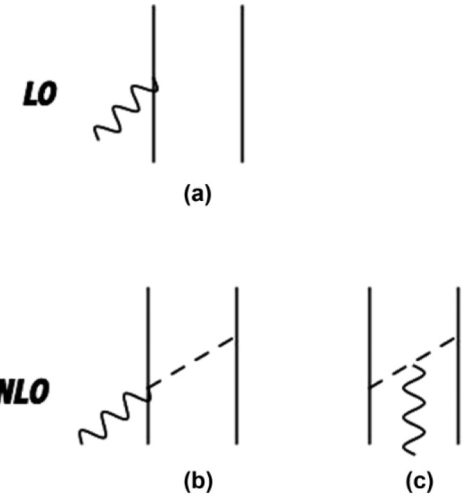
M1 moments in calcium

$$\mu_{\text{NLO}}(k) = -\frac{i}{2} \nabla_q \times \mathbf{J}_{1\pi}(q, k) |_{q=0} + \frac{i}{2} e (\boldsymbol{\tau}_1 \times \boldsymbol{\tau}_2)_z \mathbf{R} \times \nabla_k V_{1\pi}(k)$$

“Intrinsic”

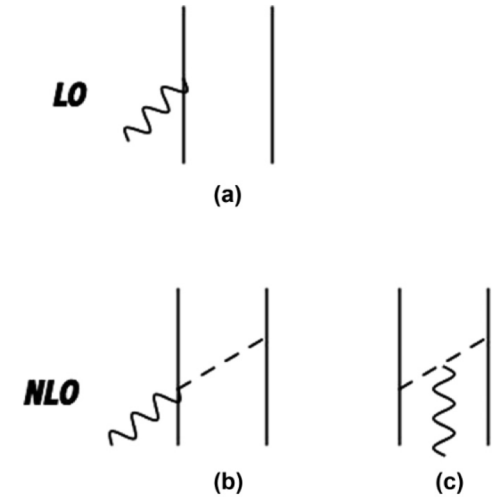
“Sachs”

Sachs term give dominant contribution

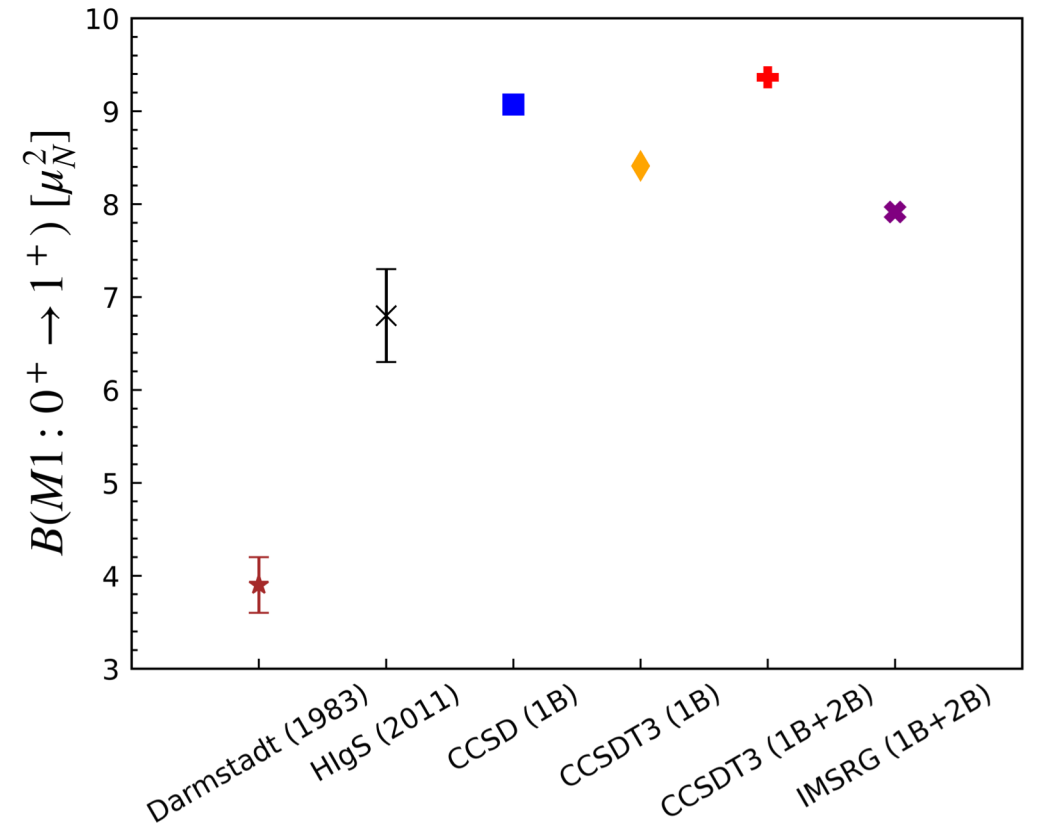
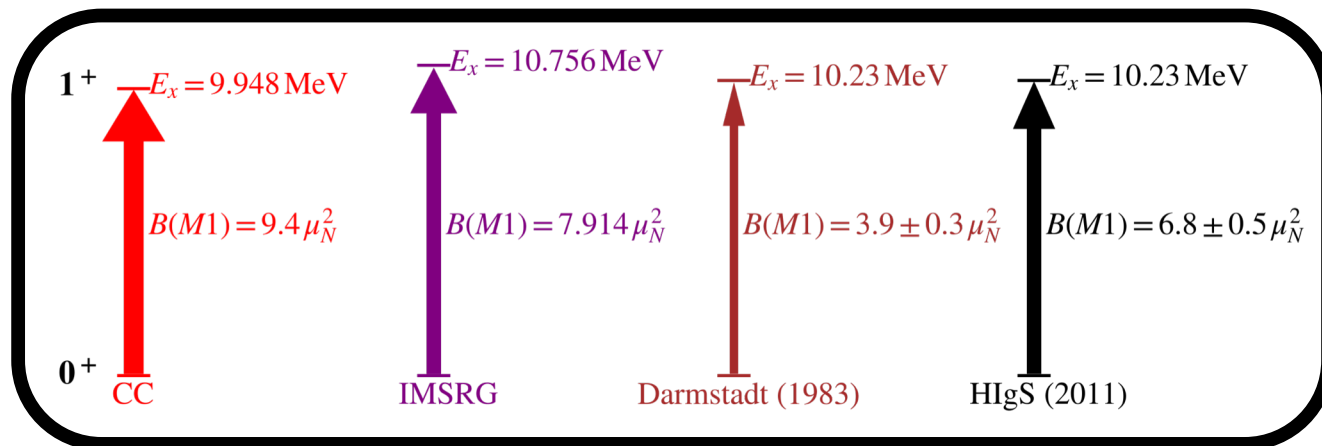


M1 transition in ^{48}Ca

$$\mu_{\text{NLO}}(k) = \underbrace{-\frac{i}{2} \nabla_q \times \mathbf{J}_{1\pi}(q, k)|_{q=0}}_{\text{"Intrinsic"}} + \underbrace{\frac{i}{2} e(\boldsymbol{\tau}_1 \times \boldsymbol{\tau}_2)_z \mathbf{R} \times \nabla_k V_{1\pi}(k)}_{\text{"Sachs"}}$$



- Sachs operator gives dominant contribution
- Instead of quenching, 2B currents actually enhance $B(M1)$, consistent with I. S. Towner, Phys. Rep. 155 (1987) 263



Summary

- Projection after variation coupled-cluster theory with improved left state and three-nucleon forces yield accurate descriptions of rotational structure of neon isotopes: ^{34}Ne as rotational as ^{32}Ne and ^{34}Mg
- Using history matching, Bayesian methods and emulators predict ^{28}O to be unbound with 98% certainty
- Developed accurate emulators of symmetry projected Hartree-Fock which opens a way to link nuclear deformation to underlying microscopic nuclear forces
- Deformation in neutron rich neon isotopes is correlated with the amount of attraction in the 1S_0 partial wave
- This picture was found to be consistent with a global sensitivity analysis of the R42 ratio on the low-energy constants of Delta-full NNLO interaction

Thank you for your attention!